

1 **Evidence and causes of strong ocean heating during glacial periods.**

2

3 **Sergey A. Zimov, Nikita S. Zimov**

4 North-East Scientific Station, Russian Academy of Sciences

5 Malinovii yar 3, Cherskii, Yakutia, Russian Federation, 678830

6 nzimov@mail.ru

7

8

9

10

11

12

13

14

15

16

17

18

19

20

21

22

23

24

25 **Abstract**

26 We investigated data from all initial reports of deep-sea drilling projects and have noticed
27 that on the surface of the ocean bottom geothermal heat flux is approximately 40 mW/m^2 higher
28 than hundreds meters below. This infers that during the last glacial period interior ocean temperature
29 was warmer than it is today.

30 What phenomena can cause interior waters warming? The densest water in the world's
31 oceans exists in the Red Sea. Under current conditions the Red Sea is slowly pumping salt down
32 into the ocean interior and freshening the surface. Presented here model of thermohaline circulation
33 is showing that this decrease density of water in the high latitude seas and in 1600 years northern
34 downwelling ceases. This indicates the beginning of a new glaciation. The ocean becomes strongly
35 stratified and only warm-dense water from the Red Sea is filling it. Additional heating to the ocean
36 is given by the geothermal heat flux and organic rain decay. According to our calculations in 112000
37 years, temperature of the water in the ocean interior reaches 23.4°C and becomes less dense than the
38 water in the high latitude seas. This causes strong convection to occur. Water temperature in the
39 Northern Atlantic increases by 18°C . Rapid glacier degradation occurs as the ocean quickly releases
40 accumulated heat and in 14600 years ocean interior drops to 1.6°C . After this period a new
41 glaciation cycle starts. In our model energy input from space and earth interior is set constant but we
42 still received asymmetrical glacial cycles.

43

44

45

46

47

48

49

50

51

52 **1.1. Introduction**

53 Numerous hypotheses have addressed glacial-interglacial climatic dynamics, but none of
54 them explain the sharp 25⁰C temperature increase in Greenland in the last deglaciation [Cuffey et
55 al., 1995; Dahl-Jensen et al., 1998]. These robust data were obtained through analyzing the
56 temperature profile in the Greenland ice sheet where cold from the last glaciation is preserved in the
57 depth of the glacial sheet [Cuffey et al., 1995; Dahl-Jensen et al., 1998]. Approximately the same
58 temperature rise was shown by data about the extent of vast Late Pleistocene ice wedges on the
59 plains of western Europe [Washburn, 1979]. Such large ice wedges occur only in extremely cold
60 environments where the average annual temperature is below -12⁰C [Washburn, 1979]. Currently
61 mean annual air temperature there is around +10⁰ C.

62 Planet orbit oscillations, changes in global albedo and increases in greenhouse gas
63 concentrations are all relatively slow processes. However, the Greenland data indicate that climate
64 changed instantly. In Greenland, ice cores reveal that until ~14650 years ago, there were no
65 substantial fluctuations in climate [Severinghaus and Brook, 1999]. The annual accumulation of
66 ~100 mm of snow contained relatively stable isotopic content. This signal changed sharply along
67 with the extreme temperature perturbation. The thickness of annual ice layers doubled stepwise over
68 3 years as well [Severinghaus and Brook, 1999]. Then, during Younger Dryas, the climate changed
69 back to glacial conditions, but ~11700 years ago a new sharp shift in climate occurred [Severinghaus
70 and Brook, 1999]. It can be supposed that because of glacier retreat, change in albedo and increased
71 emission of greenhouse gases, the temperature in northern latitudes should grow with the course of
72 deglaciation. But data of the temperature profile in the Greenland ice sheet clearly show that the air
73 temperature on the surface of the ice sheet has, in contrast, declined by 2.5⁰C [Dahl-Jensen et al.,

74 1998]. Therefore, this 25 degrees heating happened stepwise; and the highest air temperature was at
75 that moment.

76 Ocean surface circulation can change in one year, but that would only cause redistributions
77 of solar energy over the ocean surface. In order to increase the temperature in the northern Atlantic
78 and surrounding lands by 25⁰C, in some other big territories the temperature should drop
79 respectively. 25⁰C is a huge change, analogous to the difference in average annual air temperatures
80 between the Arctic and the tropics. Such an increase is impossible to explain in the frames of
81 existing knowledge about earth's climate system. For that, an additional energy source is required.
82 There are many natural phenomena which display sharp asymmetric cycles similar to the glacial-
83 interglacial cycles. Most frequently they are based on slow energy accumulation and consequent
84 quick release [Chuprynin, 1985]. Such an accumulator could be the world ocean.

85 We suggest that during glaciations the ocean accumulated energy: interior ocean water
86 heated up to ~20-30⁰C and during deglaciation this energy is released. Here we consider reasons and
87 evidences for the phenomenon.

88

89 **1.2. Warm ocean hypothesis**

90 The heaviest water is on the bottom of the ocean. Currently the ocean is filled with cold and
91 therefore heavy (1027.8 kg/m³) water from high-latitude seas. The salinity of the water is 34.7‰
92 [Hay, 1983]. But that is not a single and moreover rather rare scenario in the history of the ocean
93 [Hay, 1983]. In the past, in warmer climates, the ocean was filled with heavy but warm water from
94 seas with high evaporation [Hay, 1983]. Today there are two such seas (plus the Persian Gulf). First,
95 the Mediterranean Sea, because of the difference in evaporation and precipitation where every year
96 on average 850 mm of water is lost. Through Gibraltar straight 42320 km³/yr of ocean water enters
97 the Mediterranean while 40800 km³/yr bottom flow leaves this sea with 38.4-38.7‰ salinity, and a
98 temperature of 12.5⁰C [Hay, 1983]. Annual evaporation from the Red Sea is 3500mm of water.

99 From it, 9400-12600 km³/yr of water with a salinity of 41.5‰ and temperature of 22.5°C flows
100 down to the abyssal depths of the Indian ocean [Hay, 1983]. The densest water of the world ocean
101 (1028-1029 g/m³) flows out of these seas [Hay, 1983]. Both the Red and the Mediterranean seas are
102 very deep and connect to the ocean by shallow straits. They can be considered as “small oceans”,
103 and they can be used as examples of warm ocean interior waters [Hay, 1983]. They are filled with
104 warm water throughout their whole depth. On the bottom of these seas, the temperature is 12.6-
105 13.4°C and 22.5°C [Hay, 1983]. Today the total flow from these salty seas into the ocean interior is
106 only several per cent of the flow from high-latitude cold seas [Hay, 1983]. Therefore their effect on
107 ocean interior temperatures is minor; because of their influence ocean bottom temperatures are not
108 0°C but +2°C [Hay, 1983]. If one imagines these seas as water pumps, then these pumps have low
109 power (debit). But these haline pumps give stronger pressure (density of water), therefore they are
110 stronger than thermo pumps of the high-latitude seas. Their debit is small compared with a thermal
111 pump, but the stream from the Red sea would fill the whole of the world ocean volume in 100,000
112 years, i.e. for one glacial period. Flow from the Mediterranean Sea would fill the world ocean 4
113 times faster.

114 One very important phenomenon is connected with the function of such haline pumps: they
115 reduce the salinity of the ocean surface and compete both with thermal pumps and between
116 themselves. They pump salt down to the ocean bottom and fresh water evaporated from these seas
117 comes back to the ocean surface. They pump down the ocean bottom water with high salinity and
118 instead somewhere in the world ocean appears a compensating flow from the depth to the surface
119 with 34.7‰ salinity. While thermal pumps strongly mix the ocean, this process is barely noticed, but
120 if thermo pumps weakened an irreversible freshening of surface waters would begin. One possible
121 trigger for this can be, for example, the melting of glaciers and short-term freshening of the ocean
122 surface [Hay, 1983]. The density of this water would reduce and the downflow of cold water would
123 stop [Hay, 1983]; the haline pumps would continue to work thereafter; haline pumps would quickly

124 make the surface water even fresher. Water in cold seas becomes lighter and would not yet be able
125 to submerge. The ocean would become strongly stratified; wind and tides would not be able to mix
126 this water with heavy bottom waters. As a result, haline pumps would pump warm and salty water
127 onto the ocean floor without interference.

128 Another possible reason for ocean interior waters to warm is geothermal heat flux. Energy of
129 50mW/m^2 is sufficient to warm an entire ocean water column (4km) during one glacial cycle
130 (100,000 years) by 10^0C [Adkins et al., 2005]. Another mechanism is biological heating. About 11
131 Pg (1 Pg= 10^{15} g) of organic matter (representing about one-quarter of the ocean bio productivity)
132 descends annually to the ocean interior and the bottom [Chapin et al., 2002]. Only 2% of the value is
133 buried in the bottom sediments [Chapin et al., 2002]. Taking into account the ocean area of $0.361 \times$
134 10^{15}m^2 , on average, about 30 g of carbon (or ~60 g of organic matter) is oxidized on each square
135 metre of the ocean floor annually. Heat flow of 40mW/m^2 is computed using an average 5 kcal/g
136 (21 kJ/g) energy content of 'sea food'.

137 **2.1. Proof of ocean heating in the glaciations**

138 The conclusion that thermal convection in the glacial ocean (ocean ventilation) was
139 significantly reduced is based on a big difference between the ^{14}C age of planktonic and benthic
140 foraminifera [Sarnthein, 2011]. The same conclusion was based on the tenfold increase in
141 productivity in the Southern Ocean during the last deglaciation [Anderson et al., 2009]. Because of
142 increased circulation, the nutrition supply from the interior to the ocean surface has sharply
143 increased [Anderson et al., 2009].

144 The most exact data of surface ocean salinity in the last glaciation are obtained through
145 analysing plankton fauna in deep boreholes of the north-western Atlantic and numerous samples
146 obtained for recent complexes of these species from different basins in northern Atlantic and the
147 Arctic [de Vernal and Hillaire Marcel, 2000]. Before the peak of glaciation, huge masses of fresh ice
148 were accumulating on land and on sea surfaces, and water salinity should have been expected to rise

149 at that time. However, on the north-west Atlantic both before and during the last glacial maximum
150 (LGM) it was 30-32‰ [de Vernal and Hillaire Marcel, 2000]. Same analyses can't be conducted for
151 other regions, since for comparison fauna from seas with low salinity are needed, while such seas
152 exist only in the north. The northern Atlantic is an open ocean. Water on the surface of the world
153 ocean is mixed quickly. From this it follows that on the entire ocean surface in LGM salinity was
154 ~3-5‰ lower than today. We have received the same value in our model (see below).

155 Even cold water with such salinity is very light. No tides or winds can submerge such water
156 to the ocean floor. Geothermal energy and biogenic heating are real phenomena. If the entire ocean
157 was strongly stratified, then there would have been no vertical mixing. Diffusion heat losses are
158 minor, therefore these two sources must have warmed the ocean interior.

159 If the ocean surface was freshening, then on the ocean interior salinity must have risen. And
160 this anomaly must have persisted in the depth of the bottom sediments. And in truth, in various
161 regions of the ocean high-salinity pore water was detected. This allowed water salinity to be
162 estimated on the ocean bottoms in the LGM. It appeared to be anomalously high – ~36.5‰ [Adkins
163 et al., 2002]. Such salinity can't be explained solely by glacier growth [Adkins et al., 2002].

164 If the temperature and salinity of water on the ocean bottom in the past often and strongly
165 changed (during all glacial cycles), then benthic organisms should be resistant to these changes. This
166 is supported by the present distribution of foraminifera on the ocean floor. This is indeed not
167 connected with temperature and salinity and depends on food supply [Van der Zwaan et al., 1999]
168 The same species can now be found both in the warm bottom of the Red Sea and in the cold bottom
169 of the Norwegian Sea [Badawi et al., 2005].

170 Our hypothesis supposes that in the LGM the ocean floor was filled with warm water from
171 the Red Sea. This means that the temperature and $\delta^{18}\text{O}$ of water on the bottoms of all oceans should
172 be close to those of the Red Sea. That means that benthic foraminifera $\delta^{18}\text{O}$ should be close as well.
173 Analyses of $\delta^{18}\text{O}$ of benthic foraminifera showed that on the warm bottom of the Red Sea in the

174 LGM $\delta^{18}\text{O}$ was $+(4.7-5.5)\%$, the same as in the bottom of all other oceans and the same as $\delta^{18}\text{O}$ in
175 plankton foraminifers of the northern part of the Red Sea where deep water forms [Luz and Reiss
176 1983; Hemleben et al., 1996; Geiselhart, 1998; Badawi et al., 2005]. This confirms that water from
177 the Red Sea had spread along the bottom of all oceans.

178 And now let's discuss the same fact but assuming that the temperature on the ocean floor in
179 LGM was close to freezing everywhere. Then it appears that the $\delta^{18}\text{O}$ paleothermometer is not
180 always correct. For the LGM it shows the same signal both for the cold ocean and for the warm Red
181 Sea. It is possible that biological fractionation of isotopes on the ocean floor at high temperature and
182 salinity, poor food and oxygen source and high carbonate ion concentration differed from the
183 present. Carbonate composition of benthic foraminifers' shells in the LGM likely also differed from
184 the present. Possibly, for the LGM ocean floor condition, it should be used not calcite scale of $\delta^{18}\text{O}$
185 paleo thermometer, but aragonite scale.

186 Beside that, the $\delta^{18}\text{O}$ paleothermometer doesn't account for water fractionation in the Red
187 Sea. Isotopically light water evaporates there and returns to the ocean surface with precipitation,
188 while isotopically heavy water submerges to the ocean floor. Today this process is hard to detect,
189 but in the LGM, when ocean mixing was low, this was an important factor. The same with salinity:
190 because of fractionation in the Red Sea, $\delta^{18}\text{O}$ on the ocean floor in the LGM was higher than on
191 average in the world ocean, and on the surface it was lower. (Below we will provide a new estimate
192 of water temperature on the shelf of New Zealand in the LGM. Based on this, the ocean surface was
193 cooling as strongly as terrestrial regions did). Below we will return to the $\delta^{18}\text{O}$ paleothermometer.

194 Another paleothermometer is based on the ratio between Mg and Ca in shells. Dependence of
195 this thermometer on temperature is a matter of debate. This paleothermometer often shows either
196 high temperatures in the ocean interior in the LGM [Bryan and Marchitto, 2008] or a complete
197 disconnection with temperature [Bryan and Marchitto, 2008; Yu and Elderfield, 2008]. We are not
198 going to discuss this method in more detail here. We have a more reliable method to measure

199 temperature on the ocean bottom in the LGM. This can be done by directly measuring temperature
200 in the bottom sediments in the deep boreholes.

201

202 **2.2. Deep borehole paleothermometer**

203 If for an extended period of time the temperature on the bottom was high, then bottom
204 sediments must have warmed as well. When cold water penetrates to the bottom, sediments will start
205 to cool. The top 5 meters will cool quickly – within a year, sediment layers 10 times thicker (50m)
206 will cool 100 times longer, while 500 meters will cool for 10,000 years [Yershov, 2004].

207 The cold have persisted at a depth of the Greenland ice sheet from the last glaciation. This
208 allowed the temperature on the surface to be estimated accurately in the LGM [Dahl-Jensen, 1998].
209 If in the LGM the ocean bottom was 25-30⁰C warmer than in the bottom sediments in the depth of
210 hundreds of meters this heat must have persisted. Detecting this anomaly by looking at the
211 temperature profile and estimating the temperature dynamic in the past is easier for the ocean
212 borehole than glaciers. In glaciers, active snow accumulation takes place, glaciers flow and all that
213 should be accounted for in the calculations. On the ocean floor, sediments usually accumulate
214 slowly, usually parts of a millimeter per year. Sediments stay intact.

215 Now nobody is assuming that the ocean bottom in the LGM could be warm. But 40 years
216 ago when *Glomar Challenger* was just starting to drill the boreholes, this was actively discussed
217 [Erickson et al., 1975]. By that time over 3,000 measurements of heat flux through the ocean floor
218 had been made, and it was necessary to find out whether all this flux is coming from deep crust
219 interior or this is mostly the release of heat which was accumulating during the last ocean warming
220 [Erickson et al., 1975]. In the deep boreholes it was easy to measure. If there was no change in water
221 temperature in the past then heat flux in all boreholes should not change with depth and should be
222 equal to geothermal heat flux [Erickson et al., 1975] (heat flux is calculated as a multiplication of
223 the heat-conductivity coefficient by temperature gradient [Erickson et al., 1975]); and if in the last

224 glaciation the ocean was warmer, then heat flux should be maximum at the bottom surface and
225 decline with depth in bottom sediments [Erickson et al., 1975]. Only at the big depth the flux should
226 be equal to the geothermal heat flux [Erickson et al., 1975]. At the bottom surface, the flux of
227 cooling sediments should be added to the geothermal flux [Erickson et al., 1975].

228 The Atlantic, Indian and Pacific oceans connect by deep and wide straits. Therefore, water in
229 these oceans had and now has similar temperature [Hay, 1983]. In such a case there is no need for
230 many deep boreholes to test this hypothesis. Even one accurately measured heat flux profile is
231 enough (for example, as for temperature reconstruction in Greenland). If the temperature of the
232 ocean in the past didn't change substantially, then all boreholes should show stable with depth heat
233 flux [Erickson et al., 1975]. And if in the LGM the ocean was 25-30⁰C warmer than in all boreholes,
234 heat flux at depths should be by several tens of mW/m² lower than at the ocean bottom surface
235 [Erickson et al., 1975].

236 In the frames of the Deep Sea Drilling Project (DSDP), *Glomar Challenger* has done 96 legs;
237 the heat flux profile was measured in numerous deep boreholes in the different parts of the world
238 ocean, and as noted in the final reports [Erickson et al., 1975; Hyndman et al., 1987], heat flux was
239 constant with depth. This means that the temperature of the ocean interior didn't vary substantially
240 in the past, and the observed heat flux at the ocean bottom is a geothermal heat flux [Erickson et al.,
241 1975; Hyndman et al., 1987].

242 As far as we know after publication of these authoritative papers, possible ocean interior
243 warming in the LGM was not discussed further in the literature. Stability of temperature in the
244 bottom in the Pleistocene has become a well-proven scientific fact. Models of ocean circulation,
245 climate, global carbon cycle and models of convection in the mantle were made based on this fact.
246 However, we critically read these final reports [Erickson et al., 1975; Hyndman et al., 1987] and in
247 addition carefully investigated numerous initial reports of the DSDP, which were used in the
248 preparation of final reports, and have found striking discrepancies.

249 Geothermal measurements made from the *Glomar Challenger* over the first 5 years of the
250 DSDP to leg 26 have been reviewed by Erickson et al. [1975]. The main goal of the review was to
251 find out whether these data correspond with depth geothermal heat flux, if it wasn't biased with
252 Pleistocene-Holocene bottom water temperature dynamic [Erickson et al., 1975]. We will briefly
253 repeat the peculiarities of these investigations.

254 **2.3. Feature of heat flux measurements in the deep boreholes**

255 During the drilling of boreholes, circulation of cold water (drilling fluid) in the borehole
256 strongly changes the temperature regime of the sediments. It takes several weeks in order for the
257 water to be in equilibrium with surrounding sediments. Ocean ships cannot wait so long [Hyndman
258 et al., 1987]. Therefore temperature measurements are conducted with a down-hole temperature
259 recorder, which is put down the borehole, and using high pressure a thin probe with a temperature
260 sensor is put into the thermally undisturbed sediments [Hyndman et al., 1987]. The sensor usually
261 measures temperature every few seconds. On the data file based on temperature registration can be
262 seen as the recorder is going down the cold hole's bottom, as the temperature of the probe quickly
263 rises after the probe has penetrated the undisturbed sediments, as the temperature of the probe after
264 that slowly reaches equilibrium with the surrounding sediments (ideally reaches plateau), and then
265 as the probe is removed, and appears in cold water again. Frequently it can be seen as the probe is
266 getting heated penetrating into the dense sediments with friction, and then becomes balanced with
267 the surrounding sediments and cools down. If thermo equilibrium isn't reached over the course of
268 measurements (tens of minutes) then measurement is extrapolated up until to equilibrium values
269 [Erickson et al., 1975; Hyndman et al., 1987].

270 Having temperature measurements in different levels it is possible to calculate the average
271 temperature gradient between these levels (temperature difference divided by depth difference)
272 [Hyndman et al., 1987]. The average heat flux for each depth interval is calculated by multiplying
273 the temperature gradient in this interval and the coefficient of heat conductivity [Hyndman et al.,

274 1987]. If there are several measurements of heat conductivity in this interval then average value is
275 taken. Heat conductivity in turn is measured in cores taken on board, from the borehole [Hyndman
276 et al., 1987].

277 In the final report, Erickson et al. [1975] have provided temperature profiles of bottom
278 sediments, calculated for different hypothetical scenarios of Pleistocene-Holocene ocean interior
279 temperature dynamic. We have repeated these calculations and our profiles in general corresponded
280 with profiles presented in Erickson et al. In Figure 1A we show the temperature dynamic of bottom
281 sediments for the following scenario: at the beginning of each glacial cycle the temperature of the
282 water on the ocean bottom is equal to $+2^{\circ}\text{C}$, and then in the course of 100,000 years it gradually
283 (linearly) increases to $+32^{\circ}\text{C}$. The profile of the bottom temperatures at that time (period of
284 maximum heating) is shown with red lines. After that, the temperature of the water abruptly
285 decreases back to $+2^{\circ}\text{C}$, and sediments begin to release heat back to the water. Green lines indicate
286 the temperature profile after 11,470 years of ocean cooling and blue after 14,450 years. On the right
287 side of Figure 1A corresponding heat flux profiles for these time intervals are shown. Calculations
288 are made for 3 different values of geothermal heat flux – 0 mW/m^2 , 14 mW/m^2 and 42 mW/m^2 ;
289 constant with depth heat conductivity coefficient – $1.4\text{ mW/m}^{\circ}\text{C}$, which is the most typical value
290 (see Figure 2), and a heat capacity of $3.35\text{ J/cm}^3\text{ }^{\circ}\text{C}$, which for sediments varies in a narrow range
291 [Yershov et al., 2004].

292 In Figure 1A we see bottom sediments cooling after cooling of the ocean. Most heat is
293 released from the near surface sediments. They have cooled by 30°C quickly. Sediments at a depth
294 of 500 meters have cooled in 14,450 years by 10°C . Sediments at a 1000-metre depth have cooled
295 only by 2°C . These sediments began to cool only after 12,000 years of cold ocean. In Figure 1A we
296 see that for all 3 variants of geothermal heat flux, heat flux near the surface exceeds geothermal heat
297 flux by 35 and 44 mW/m^2 , and temperature profiles in cooling sediments have salient shapes. In
298 Figure 1C temperature profiles for the same conditions but for the stable water temperature at the

299 bottom (+2° C) are presented for comparison. In this case heat flux is constant with depth and
300 temperature profiles are straight lines. If to accept heat conductivity vary with depth then heat flux
301 will still stay constant, but temperature profiles will become curved [Hyndman et al., 1987].

302 In many regions, gas clathrates are preserved in the ocean floor sediments [Miles, 1995]. At
303 a depth of 2 km and temperature of ~17° C, gas clathrates either melt or freeze (condition of phase
304 shift). At a depth of 6 km phase shift occurs at a temperature of ~25° C [Miles, 1995]. In Erickson et
305 al. [1975] this effect has not been taken into account. If the temperature of bottom sediments has
306 been and is stable, then it should be impossible to detect gas clathrates or methane in the sediments,
307 looking at the thermal flux profile [Yershov, 2004]. It will not change with depth. However, if
308 temperatures had increased by over 25°C during the glaciation, then most of the gas clathrates
309 would have melted, and frozen back after ocean cooling. If the latter is true, then we should be able
310 to locate a boundary phase change (“permafrost floor”) at a depth of a few hundred meters and this
311 boundary should be slowly moving down (several millimeters per year). This is a full analogue of
312 real permafrost dynamic [Yershov, 2004]. During gas clathrates crystallization approximately 500
313 J/g is released [Yershov, 2004]. This is more than at water freezing. Therefore, at freezing or
314 thawing of gas clathrates releases or consumes lots of heat at its roof or foot resulting in a sharp shift
315 in the heat flow profile and a bend in the temperature profile. In Figure 1B we show profiles with
316 the same conditions as in Figure 1A, but include a third of the sediment volume as gas clathrates or
317 oversaturated with methane water. For these scenarios we have accepted 20-21°C temperatures for
318 that of gas clathrates melting (that is 3 km depth of ocean). To ease calculations, we have replaced
319 the conditions of phase change with the condition that in the range of temperatures 20-21°C the heat
320 capacity of sediments is not equal to 3.35 J/cm³°C but 40 times higher. We see that the presence of
321 gas clathrates increases the difference between heat flux near the surface and in the deeper horizons.
322 In deep sediments in this case negative heat flux may even occur (heat flux not towards the ocean
323 bottom but to the mantle) (Figure 1B).

324 The same as terrestrial permafrost, “permafrost” in the bottom sediments can be two-layered.
325 Let’s assume that the gas clathrates layer is situated at depths from 0 to 600 meters below the ocean
326 floor. At warming, 400 meters of it melts from the top and 20 meters from the bottom (because of
327 the geothermal heat flux). During the next cooling, near surface sediments begin to “freeze” anew.
328 Under this new “frozen” layer will be situated a layer of “relic permafrost”.

329 If strong ocean heating occurred during glacial periods, then bottom sediment temperature
330 profiles throughout the ocean should mirror those in Figure 1A,B. If temperature changes were less
331 than 30°C, then related heat fluxes were also correspondingly less [Erickson et al., 1975]. If the gas
332 clathrates content in sediments was less, then a leap in heat flux would be observed deeper. If
333 bottom cooling happened slowly – over several thousand years – then heat flux on the surface will
334 increase by 5-15 mW/m² as compared with Figure 1A [Erickson et al., 1975]. If the ocean
335 temperature did not change, then the profiles must be as in Figure 1C in spite of the presence or
336 absence of gas clathrates.

337 Increased flux of heat near the surface is connected with the release of previously
338 accumulated heat to ocean waters. Theoretically, the same profiles as in Figure 1A can be obtained
339 if inside these sediments other energy sources are present with a total power of tens of mW/m² (for
340 example, radioactive or biological decay). However, in reality this explanation is unlikely. Such a
341 flux can be created by tens of kilometers-thick granite strata [Pollak et al., 1993]. In the layer of
342 carbonate silts with only a few hundred meters thickness, there can’t be enough radionuclide’s to
343 maintain such a heat flux. Above we showed that the total average heat release from aerobic organic
344 decomposition on the ocean floor is 40 mW/m². But most of this heat is released at the very top of
345 the bottom sediments. Only an extremely minor part of the energy penetrates to the deep sediments,
346 and its effect can be ignored.

347 Not all boreholes can be used for paleotemperature reconstructions. For example, near the
348 rift zones heat flux is very strong – hundreds of mW/m². Precision of heat flux measurement there is

349 comparable with the value of possible change in heat flux with depth, besides that heat transport
350 there occurs not only by conductivity but also with convection [Hyndman et al., 1987; Yershov,
351 2004]. Where pore water is ascending to the surface, the temperature profile is salient; where cold
352 water is descending down the sediments, it is arched [Hyndman et al., 1987; Yershov, 2004].
353 Shallow boreholes give little information. In Figure 1A,B it can be seen that a bend in the
354 temperature profile becomes noticeable at depths deeper than 400 meters. Approximately at the
355 same depths gas clathrates boundary should be expected. Precision of heat conductivity coefficient
356 estimates usually lie within the 5-15% range [Hyndman et al., 1987]. This coefficient often strongly
357 varies with depth (see Figure 2). Therefore errors in heat flux profile calculations in shallow
358 boreholes exceed the possible effect from the temperature dynamic.

359 A series of international programs have measured deep sediment temperatures from
360 boreholes drilled throughout the world's ocean basins. These include the Deep Sea Drilling Project
361 (DSDP), legs 1-96, the Ocean Drilling Project (ODP), legs 100-210, and the Integrated Ocean
362 Drilling Project (IODP), legs 301-340. For each leg, the results of temperature, heat conductivity
363 and heat flow measurements in boreholes and geological settings were published in the
364 corresponding volumes of "Initial Reports", in the chapter dedicated to that borehole (site) and/or in
365 a special section dedicated to heat fluxes. We revised the data of all depth boreholes. All referenced
366 data of holes below are taken from corresponding initial reports.

367

368 **2.4. Results of heat flux measurements in the deep boreholes**

369 Erickson et al. [1975] reviewed data from 12 first boreholes (DSDP) from which 2 or more
370 temperature measurements were collected (plus bottom temperature data; inflection of curve is
371 visible at least by 3 points). The authors of the review took temperature data, conductivity, gradients
372 and heat flow data from the initial reports and combined them onto a sheet. We display all these data
373 in Figure 2A (sites 194-254). All black dots in that figure are taken from review tables (we changed

374 nothing in these). We excluded from the analyses only the most shallow borehole (site 209) (52
375 meters) and three shallow boreholes drilled in the rift zone of the Red Sea. They show very high
376 heat fluxes (115-300 mW/m²yr [Erickson et al., 1975]); these data are beyond the figure data range).
377 At such high and variable fluxes it is impossible to detect bottom temperature dynamics within these
378 shallow boreholes. Locations of investigated boreholes we present in figure 3.

379 Erickson et al. used part of the data from the sheet for the final heat flux graphs. We present
380 (repeat) the original data from Erickson's heat flux graph with orange outline (Figure 2A). The
381 vertical size of the outline represents the extent of the averaging interval and the horizontal size
382 presents probable error estimates made by the authors of the review [Erickson et al., 1975].

383 We initially note that in this graph, boreholes 184, 185 and the lower part of borehole 206
384 weren't included. These 3 holes are the very first boreholes, on which the heat flux profile was
385 based. They are deep (300-600 m) and all 3 indicate a several times decline in heat flux with depth.
386 These data were excluded from consideration by Erickson. And in the final graph based on which all
387 conclusions were made only shallow boreholes were included. Erickson has compared those profiles
388 with theoretical profiles (see Fig. 1A), obtained for various dynamics of bottom ocean water
389 temperature [Erickson et al., 1975].

390 Based on the data, Erickson et al. [1975] concluded: "there is no consistent indication of a
391 significant vertical increase or decrease in heat flux, such as might be caused by long-term changes
392 in bottom water temperature"; (p.2515) "the heat flux usually remains constant within the estimated
393 probable error of the individual heat flow determination with depth" (p. 2527). This conclusion
394 corresponds with the final graph. On it (everything in orange in Figure 2A) we see that three
395 boreholes have indicated decreasing heat flux with depth (206, 253, 254), and two have indicated
396 increasing heat flux with depth (214, 217). And one borehole has indicated stable heat flux with
397 depth (242). So the conclusion of Erickson may seem to correspond with the data. But firstly, the
398 lowest point for borehole 271 in the final figure of the review is a mistake (The orange dot in Figure

399 2A is a mistake). The actual value is a black dot located to the left. The value is shown both in the
400 initial report and in the review table [Erickson et al., 1975]. Therefore the heat flux in this borehole
401 in reality declines with depth and not vice versa. This drastically change the statistics – now 4
402 boreholes indicate decreasing heat flux with depth with only 1 (214) indicating increase, but the
403 authors of the review noted the anomalously high heat-conductivity coefficient in the lower part of
404 the borehole, 1.3 W/m°C (see Figure 2A). The authors suggest that: “These high conductivity values
405 may have been affected by convection of interstitial water during the conductivity measurement
406 (sediments from the lower interval were noted for their unusually high water content) rather than by
407 an actual increase in the *in situ* conductivity” (p. 2523). This site should be either excluded from the
408 analyses or its heat-conductivity coefficient should be corrected. This coefficient can be roughly
409 estimated [Schloessin and Drovak, 1977]. Heat conductivity of sediments as a first approximation is
410 combined from water heat conductivity (0.6 W/m°C) and mineral heat conductivity (1-3 W/m°C)
411 [Nobes et al., 1991; Yershov, 2004]. Therefore, the higher the water content the lower the
412 conductivity. If porosity (watering) of sediments increased with depth in the borehole (it sounds in
413 the initial report “like soup”), then most likely heat conductivity would decrease with depth [Nobes
414 et al., 1991]. Temperature gradients were constant by depth in this borehole, therefore heat flux
415 likely decreased with depth.

416 Among all of the data examined in the Erickson et al. [1975], only one site (site 242) had no
417 changes in heat flux with depth (see Figure 2A). Measurement on the site at a depth of 141 m got the
418 highest reliability grade (Figure 2A). But do not trust this. The authors of the review noted that: “our
419 error estimates are very subjective” (p.2519). Here is what we read about the measurement in the
420 initial report: “On the first run (site 242), the latching device was attached to the extender with set
421 screws to prevent the DHI (downhole instrument – Z., Z) from being pushed up into the inner core
422 barrel. The latch did not return with the DHI but was recovered as coring continued.” And further:
423 “The record for the first run (Figure 1) indicates a relatively constant temperature of 6.25°C after the

424 bottom of the hole was reached. There is no indication of heating due to friction at the pull-out.
425 These observations, coupled with the fact that the release latch on the probe came off, suggest that
426 the probe was pushed up into the inner barrel before it could penetrate the undisturbed sediment.
427 However, heat-flow calculations indicate that the temperature measured may be very near the
428 ambient temperature at that depth” (p. 349). From the description it follows that the temperature of
429 the water in the hole’s bottom was measured at a depth of 141 m, but not the temperature of the
430 undisturbed sediment. Nevertheless, the measurement wasn’t excluded from the analyses and was
431 even given the lowest error grade. This was done because at value 6.25°C heat flow calculations
432 indicate stable by depth flux. But it is impossible that the waters from an only just drilled borehole
433 are near ambient sediment temperatures as thermo equilibrium requires several weeks at least
434 [Hyndman et al., 1987]. This suggests that the temperature at this site at 141 m is significantly (by
435 several degrees) higher than 6.25°C . The dot on the left graph of Figure 2A should be shifted to the
436 right (blue line) and then the temperature gradient in the upper part of the borehole will increase,
437 decreasing in the lower part (blue arrows in Figure 2A), with a resultant decrease in heat flux with
438 depth (as represented by blue arrows in Figure 2A). The fact that the temperature measurement at
439 this point is incorrect (lowered) could be guessed by noticing the anomalously low resulting heat
440 flux in this borehole – 29 mW/m^2 [Erickson et al., 1975]. Figures 2A, B, C shows that the heat flux
441 on the floor surface everywhere exceeds 40 mW/m^2 . By increasing the temperature at the 141-metre
442 depth by several degrees we increase the heat flux on the bottom to the typical observed values.

443 Finally, we see that out of 6 boreholes presented in Erickson et al., 5 indicate approximately
444 5 mW/m^2 per hundred meters decline in heat flux. In the sixth borehole (site 214) the heat flux is
445 likely declining as well. All these boreholes are shallow and for each of them the error when
446 estimating the heat flux gradient is comparable to the values of errors obtained during measurement.
447 But 6 boreholes is already the reliable number for statistics. All these boreholes are drilled in

448 different parts of the world ocean and already, based solely on these boreholes, the conclusion can
449 be drawn that the heat flux in the bottom sediments most likely declines with depth.

450 Now let's investigate data from boreholes excluded from the Erickson et al. analyses.

451 Two deep measurements on site 206 from the Erikson et al. review indicate strong decreases in
452 heat flux with depth (Figure 2A) and were excluded from the final heat flux graphs only for this
453 reason [Erickson et al., 1975]. The authors did not believe that this is possible [Erickson et al.,
454 1975]. The quality of these measurements is far from excellent; however, as suggested by Von
455 Herzen in the initial report, the fact that two measurements from the same core show low heat flux
456 increases their reliability. This author analysed all the possible reasons that could lead to a
457 downward decrease of heat flux: internal radiogenic or biogenic heating in the upper intervals and
458 upward percolation of interstitial waters could not explain the natural patterns observed. Large
459 changes in bottom water temperatures could result in a downward decrease in heat flux, but Von
460 Herzen could not find an explanation for how such a big ocean water temperature change could
461 occur.

462 Measurements from sites 184 and 185 also indicate strong decreases in heat flux with depth
463 and were therefore considered unreliable, and thus fully excluded from further analyses [Erickson et
464 al., 1975]. However, firstly, these boreholes are deep, and when estimating errors in gradients, the
465 sum of errors in temperature measurements is divided by the difference in depth. Therefore, the
466 greater the distance between the two measurements (the deeper the borehole) the more reliably the
467 temperature gradient is likely to be calculated. Secondly, both boreholes are drilled in one place on
468 the Umnak Plateau in the Bering Sea under similar conditions. Measured heat conductivity and
469 geothermal heat flux at depth are similar in both boreholes [Erickson et al., 1975], increasing the
470 relative reliability of the measurements. Thirdly, the patterns in the data from all four temperature
471 measurements appear to be of good quality: after the penetration of the probe into the sediments the
472 temperature quickly increased before reaching a plateau in 3-4 minutes. These boreholes show

473 strong heat flux increases at 200 m deep. We see such a profile in Figure 1B. An oversaturation of
474 pore water with methane was recorded whilst drilling both boreholes. The bend in the temperature
475 profile in this “combined” borehole is located on the cross point between the temperature profile and
476 the profile of the temperature of gas clathrates freezing (Figure 2A). Most likely today, this site
477 contains gas clathrates – above this bend sits the gas clathrate horizon and below methane in
478 gaseous form.

479 We see that in Erickson’s review the heat flux data were the subject of strong selection and
480 corrections. Only deep boreholes can give reliable evidence of the Pleistocene-Holocene dynamic of
481 ocean temperatures. All of them were unreasonably excluded from the analyses. On the other hand,
482 clearly incorrect measurements, which didn’t show a decline in heat flux with depth, were given the
483 highest reliability rate.

484 In the Erickson review only the very first boreholes were included. After that, hundreds of
485 measurements were conducted, but the conclusions drawn in this review have never been questioned
486 since.

487 Now let’s analyze the final review based upon all of the boreholes of the DSDP, up to leg 96
488 [Hyndman et al., 1987]. Based on these numerous data, its authors have drawn the following general
489 conclusion: “there is no conclusive evidence of bottom water temperature changes of a few degrees
490 or more over time scales of tens of thousands of years ... this supports the initial hypothesis of
491 Erickson et al. [1975]” (p.1573). In their review, the authors present a big table containing 86 sites
492 with measurements of heat flow, which (in their opinion) support their conclusion. However, the
493 authors note that “in this data summary we have included only sediment probe heat flow values
494 having ... at least three points with interpreted equilibrium temperatures that form a uniform
495 gradient (or a constant heat flow with depth if the conductivity varies significantly). Some
496 potentially good data have thus been excluded, but we feel that these are necessary criteria to
497 establish the validity of a hole bottom temperature probe measurement” (p.1570). Thus, the authors

498 at the first stage excluded a great number of good data only because they could be indicative of
499 temperature changes of the ocean's bottom. And after the selection they draw the conclusion that
500 there is no proof of bottom water temperature changes. This is a very big methodological mistake.
501 This analysis is incorrect.

502 If the authors have previously excluded from analyses all data that indicate temperature change
503 on the ocean bottom then in their data summary among 86 sites should be many boreholes which
504 approve the conclusion about stable temperature on the bottom. But firstly, the authors of the review
505 stated that in this table only boreholes containing at least 3 measurement points were included.
506 However, half of the sites which have got into the final table have only one measurement besides the
507 bottom surface measurement. Based on these sites, the bottom water temperature dynamic can't be
508 judged. Two points can't show profile bend. Secondly, 9 sites in the review table [Hyndman et al.,
509 1987] are the boreholes from the isolated Mediterranean and Black Sea. Their temperature history is
510 not connected with the open ocean. Thirdly, the majority of the remaining sites included in the table
511 are boreholes shallower than 200 meters. They can't be reliable evidence of the Pleistocene-
512 Holocene ocean temperature dynamic.

513 We have found in the big sheet only 3 deep holes (>400 m) drilled in the open ocean in which
514 three or more temperature measurements are present and there are thermal conductivity
515 measurements (Figure 3). Of these, only one borehole is classified as having "good" quality (site
516 533), i.e. the site used by the authors to prove stability of heat flux with depth. However, as follows
517 from the measurements data, and as was noted in the initial report, these data in fact show a strong
518 decline in heat flux with depth (Figure 2B). And this isn't the casual error. The authors of the review
519 have seen that the heat flux is declining with depth and have tried to correct these data. They have
520 reduced temperature at 156 m and 256 m to 0.6°C. But this small correction does not change the
521 situation notably. The thermal flow decreases with depth anyway. In addition, that correction is
522 abusive as it was noted in the initial report that if there is a possibility of a correction, then it might

523 only be correction toward an increase of temperature on the levels. Before the temperature probe
524 was removed from the sediments, it hadn't yet reached equilibrium and temperatures still continued
525 to grow, so the researchers who conducted measurements accepted the maximum temperature
526 reached.

527 Of the remaining 2 sites, graded as "fair", site 582 also shows a very strong decline in heat flux
528 with depth (Figure 2B). We should note that the maximum methane concentration there was
529 discovered at a depth of ~300 meters. Likely, gas clathrates floor locates at this depth , and that
530 means that the temperature there is +24° C.

531 Site 397 was reported in the review as containing 3 temperature measurements. Even if only
532 these three measurements were to be considered, heat flux would still decline with depth (figure
533 2B). But in fact, 5 measurements were originally made. The lower 2 measurements were excluded
534 from the review analyses. But these are the most interesting measurements. Measurements at a depth
535 of 1438 m gave a downhole temperature of 21-27 °C. The precision of these measurements is very
536 low, but the fact that this measurement is close to being real value is supported by measurements at
537 depths of 448 and 579 meters. They have high quality and show negative heat flow (Figure 2B). In
538 Figure 1,B we see that this is possible at sharp temperature changes on the ocean's floor at low
539 geothermal flow. As it noted in the initial report, these sediments are rich with methane. The
540 theoretical floor of gas clathrates is situated exactly at the bend in the temperature profile (Figure
541 2B). It is therefore likely that this represents a situation as presented in Figure 1B.

542 Finally, all three deep sites that were included in the review analyses to prove stable heat flux
543 with depth in truth do not show this; they show a sharp decline of heat flux. We have restricted our
544 analyses and have shown on the Fig. 2B,C only boreholes with depths >400 m, but a similar picture
545 can be seen in data from shallower boreholes. For example, in the final table only 1 borehole (335)
546 exists in the range 300-400 meters [Hyndman et al., 1987]. It has "excellent" quality on the sheet,
547 i.e. it states that it reliably proves the cold ocean hypothesis [Hyndman et al., 1987]. But, as seen in

548 the initial report , it also clearly shows a decline in conductive heat flux with depth. In this table all
549 shallow boreholes from the Erickson report are included as proof of the stable heat flow, but as we
550 showed earlier, all of them show heat flux decline with depth.

551 Now let's investigate the data of deep (>400 m) boreholes which were not included in the final
552 table in the review, but were noted in the Appendix [Hyndman et al., 1987] (see Figure 2B). Besides
553 the already mentioned site 185, there is also site 406 (Figure 3). It is presented in the table but only
554 as a shallow borehole with 4 measurements. In truth, it was a deep borehole with 6 temperature
555 measurements showing a decline of heat flux with depth (Figure 2b). At site 549 there was not only
556 2 measurements, as noted in the table, but 3, and there were heat flux declines there with depth as
557 well. Site 568 was excluded from the table, but noted in the Appendix. There the heat fluxes
558 declined also. The temperature profile of this borehole reached the bottom of gas clathrates (Figure
559 2b). This is validated by the drilling results. Gas clathrates were detected from this borehole at 190-
560 315 m and 391-410 m depths (these gas clathrates were taken up on board). Below 410 meters, as
561 drilling showed, gas is in a nonhydrated state. If 1 more temperature measurement below this depth
562 had been conducted in this borehole then a sharp shift in the heat flux would likely have been
563 obtained.

564 We checked all of the deep boreholes from the open ocean DSDP drilling program and found
565 total discrepancy between the conclusion of the final review and the facts. Even careful data
566 selection could not hide this. All the boreholes show that strong heat flow decreases with depth.
567 There are no data proving the cold ocean hypothesis.

568 It should be noted that the authors of measurement have always seen heat flux decline with
569 depth. The fact that the actual data contradict the accepted hypothesis has always troubled them. In
570 most cases it is briefly noted in initial reports. But this topic is never deeply discussed.

571 Now let's investigate boreholes drilled in isolated basins – the Mediterranean and Black seas.
572 There are 3 such deep boreholes contained in the table of the review: site 374 – 304 m, site 379 –
573 425 m, and site 380 – 370 m [Hyndman et al., 1987]. All of them have “excellent” quality. Their
574 high quality is especially noted in the review [Hyndman et al., 1987]. They differ from boreholes in
575 the open ocean by displaying stable heat flux. These measurements indicate that water temperatures

576 in the bottom of these seas during the late Pleistocene differ not much from modern day (12.5°C and
577 9°C).

578 In reviews based on DSDP results [Erickson et al., 1975; Hyndman et al., 1987], deep
579 temperature measurements were excluded from analysis. In following drilling projects such deep
580 measurements became very rare. Among initial ODP and IODP reports we found only 4 deep
581 boreholes in open ocean that have temperature measurements in undisturbed sediments deeper than
582 400 m. Let's investigate these boreholes. What is interesting is that the temperatures in these
583 boreholes were measured not only by temperature probe but with other methods too.

584 In a united 671-948 borehole, measurements were conducted during legs 110 and 156. The
585 combined results are presented in Figure 2c. (We have corrected one obvious mistake made at
586 temperature extrapolation at a depth of 247m.) The temperature gradient below 100 m stays almost
587 stable and a decline in heat flux with depth occurs due to the reduction in heat conductivity. On the
588 same site in parallel borehole 948D temperature loggers were installed. In 18 months, when
589 borehole temperatures stabilized, they indicated approximately the same result – a stable
590 temperature gradient (72°C/km) below 100 meters. This proves the reliability of the old technique.

591 At site 704 a decline in heat flux with depth was recorded (Figure 2c). Additionally, the
592 temperature profile was calculated based on the porosity and resistivity of sediments at this site. It
593 also showed a strong decrease in thermal flux with depth [Nobes et al., 1991].

594 On site 801 during leg 144, 2.5 years after drilling, the temperature profile was measured in
595 detail. Data on the heat flux from this borehole are likely to be the most reliable of all. The decline
596 in heat flux with depth found (Figure 2C) strongly correlates with model results (Figure 1A).

597 In borehole 1093 the heat flux also declined. Numerous measurements in the upper interval
598 were conducted with limited distance between them, increasing errors in heat flux. If you average
599 these data, then the decline of heat flux with depth becomes obvious. Importantly, although the

600 measurement quality at the site was low, the most important measurement in this borehole (depth of
601 482 m) was made with “excellent” quality.

602 Borehole 1226 has crossed the line of stable gas clathrates at 305 m depth, and exactly at this
603 point there is a sharp bend in temperature profile (Figure 2c). This may indicate the borehole
604 piercing a low-power gas clathrates horizon. This is evidenced by high methane concentrations and
605 a clear peak in the velocity of p-waves at this depth.

606 Now we investigate boreholes of isolated seas and shallow water. The Pleistocene-Holocene
607 dynamic on the bottom should differ there from the open ocean bottom water. Borehole 1352
608 drilled on the continental border 60 km east of New Zealand to a depth of 344 meters is the only
609 deep borehole which indicated heat flux increase with depth (Figure 2C). This means that in this
610 region during the peak of glaciation, when New Zealand was covered with glaciers, water surface
611 temperatures were close to zero (today $\sim 9^{\circ}\text{C}$).

612 The Japan Sea freezes in the winter; it is connected to the ocean by only shallow straits.
613 During legs 127 and 128, 5 boreholes were drilled to depths of 130 to 300 meters. All of them
614 showed precisely uniform profiles of temperatures and stable heat flow. This means that bottom
615 temperatures were stable ($\sim 0^{\circ}\text{C}$) both in glacial periods and today.

616 Borehole 1324 was drilled to the north of the Mexican Gulf at a depth of 1057 m. This site
617 displays complicated bottom water temperature dynamics. In the upper part of this borehole a
618 temperature gradient of $\sim 100^{\circ}\text{C}/\text{km}$ was measured, which then declined to $18.6\text{-}21.3^{\circ}\text{C}/\text{km}$. Deeper
619 than 300 m it declined further to $16.2\text{-}16.7^{\circ}\text{C}/\text{km}$, and below 530 m it will likely rise again. Today at
620 a depth of 1 km in the North Atlantic, water temperatures are $6\text{-}10^{\circ}\text{C}$, largely from Mediterranean
621 Sea waters [Hay, 1983]. But the temperature at the ocean’s bottom of site 1324 is $+2^{\circ}\text{C}$, meaning
622 that there is an influence of water from Arctic seas. Possibly, initial Holocene bottom waters at this
623 site were cold, then they were penetrated by Mediterranean waters before Arctic waters penetrated
624 once again.

625 We have analysed all of the temperature measurements from sediments of deep oceanic
626 boreholes. However, boreholes drilled in young ocean floor basalts also exist. Unfortunately, the top
627 layer of young basalts is highly permeable and when they are pierced with a borehole, the flow of
628 cold heavy water inside the borehole takes place [Hyndman et al., 1987]. Even a weak flow
629 significantly changes the temperature profile: it becomes concave and smooth; it does not have
630 bends which have to exist in places of sharp thermal conductivity changes (for example, site
631 1309D).

632 The most intensively studied basalt borehole is 504. It is the deepest borehole (2111 m) and
633 contains detailed heat-conductivity measurements as well as permeability measurements. In the
634 upper part of basalts, permeability is 10^{-13} m^2 , and water flows into the borehole there. By 536 m
635 depth, permeability decreases to 10^{-17} m^2 and water filtration is impossible below this point. These
636 basalts are 5.9 million years old. On top they are covered with a 275-metre-thick layer of sediments.
637 The heat flux measured in these sediments is equal to 196 mW/m^2 . This corresponds with
638 measurements made on bottom surfaces conducted in the area around this borehole. High-precision
639 temperature measurements were conducted in this borehole during legs 92, 111, 137, 140 and 148.
640 All measurements indicated that the conductive heat flux in basalts calculated through a temperature
641 curve declined from $180\text{-}200 \text{ mW/m}^2$ at 550 m to $120\text{-}125 \text{ mW/m}^2$ at 1000-metres depth, and
642 remained the same down to the bottom of the borehole. This is a very strong and reliable
643 measurement of heat flux decline with depth, therefore several duplicating measurements were
644 conducted, but all of them have indicated the same thing. All possible reasons for such a strong
645 decline in heat flux (except for changes of bottom temperatures) were considered in detail (Initial
646 Report, Leg 111). But a convincing reason was not provided. One potential explanation suggested
647 that heat conductivity in basalts can increase with increasing pressure and temperature, and for
648 values measured on board the ship should be made a correction for *in situ* conditions (leg 92).
649 However, special investigations showed that this explanation doesn't help – pressure influence is

650 minor, and with temperature increase heat conductivity within the temperature range 28-170°C does
651 not increase but declines by 0.0054-0.01 W/m °C for each degree of temperature rise [Schloessin and
652 Drovak, 1997]. This phenomenon is more likely a general rule for crystal geological material; the
653 only exclusion from this rule is glassy (amorphous) basalts [Petrunin et al., 1971; Schloessin and
654 Drovak, 1997]. Experiments on sedimentary samples from hole 549 (calcareous silty mudstone,
655 calcareous sandy mudstone, sandy limestone and sandy siltstone) indicate a significant decrease in
656 conductivity also by between 0.007 and 0.011 W/m °C per degree over the temperature range zero to
657 80°C [Foucher et al., 1984].

658 For deep and hot boreholes it is a very strong correction; because of it, the heat-conductivity
659 coefficient and calculated heat flux can be reduced twice. For deep boreholes in unconsolidated
660 sediments this correction is also valuable, since sediments compress with depth. Analysing data
661 from boreholes, this important correction was never applied, since it just strengthens the heat flux
662 decline with depth, which, it is broadly considered, cannot happen. In contrast to mineral carcass,
663 thermal conductivity of interstitial water increases with temperature rise [Erickson et al., 1975]. The
664 correction mitigates thermal flow decrease by depth. Therefore it has always been done in full
665 strength [Erickson et al., 1975; Hyndman et al., 1987], even when sediments' porosity and
666 temperature gradient strongly decrease with depth.

667 3. Results

668 In the final reports it was announced that heat flow on the bottom of all oceans does not
669 change with depth and therefore temperature on the ocean floor didn't differ much in the Pleistocene
670 [Erickson et al., 1975; Hyndman et al., 1987]. But we have checked all deep open ocean boreholes
671 and did not find evidence of that. In contrast, a sharp decline was observed in all holes (Figure 2).
672 We can see the decrease of heat flow in the shallow boreholes and in the upper parts of the deep
673 boreholes too (Figure 2). In boreholes 504, 801 and 948 temperatures were measured precisely (in
674 detail) inside the borehole after they had reached heat equilibrium, and in all of these boreholes a

675 strong decline of heat flux with depth was observed. All deep boreholes of the open ocean have
676 indicated similar declines in heat flux with depth. We see that heat fluxes on the ocean floor are at
677 least 40mW/m^2 higher than geothermal flux. If there is a bend in a temperature profile, then it
678 corresponds with the boundary of stable gas clathrates (184, 397 and 1226) (Figure 2). Such results
679 could not be just chance. In isolated seas, in which the Pleistocene-Holocene temperature dynamic
680 was minor, heat flux stays constant with depth, and in shallow waters, where in the LGM water
681 temperature was lower than today, heat flux grows with depth. This means that most temperature
682 measurements were in truth done reliably and reflect the actual situation. These data give much
683 interesting information.

684 We reached our conclusion of a heat flux decline with depth not by using statistical methods or
685 averaging data sets, but from analysing each borehole. The conclusion of a 25°C temperature change
686 in Greenland was based upon evidence from one core, yet we base our conclusion on numerous
687 cores and all of them without a single exclusion indicated that the ocean floor in the LGM was
688 warm. Subjective factors had a minor effect on our conclusions. We didn't conduct any
689 measurements ourselves, taking all data from initial reports. The authors of these measurements
690 were sure that heat flux is stable with depth. The subjective factor favored the cold ocean
691 hypothesis.

692 The heat flux profile in bottom sediments is the most simple and reliable paleothermometer. It
693 is based on a simple physical law – Fourier's law: heat flux is proportional to temperature gradient.
694 We have tested the reliability of this paleothermometer on the ocean floor, in the Mediterranean,
695 Black and Japan seas, and on the New Zealand shelf. It works everywhere reliably. We have
696 confidence in it. The temperature profile shows the temperature itself – heat that is preserved in the
697 sediments from the previous warming. All other paleothermometers are not connected with
698 temperature directly. They are analysing some parameters which are connected with temperature.

699 These are empirical dependencies, and there is no confidence that these dependencies account for all
 700 factors.

701 At the moment we are not trying to reconstruct the last ocean cooling in great detail. Did cold
 702 water penetrate the Atlantic and Pacific interiors simultaneously? When did the strongest
 703 overturning occur, in Bølling-Allerød or after Younger Dryas? Yet, by comparing measured
 704 temperature profiles (and especially the profile of site 801) (Figure 2) with modelled ones (Figure 1)
 705 we see that ocean floor heating was strong, 25-30°C. Only such a heating would cause gas clathrates
 706 to melt, and at their second freezing sharp bends would occur in temperature profiles.

707

708 **3.1. Geothermal flow**

709 In theory, as the lithosphere cools (moving away from rift zones), heat flux must decline
 710 proportionally to the square root of crust age [Stein and Stein, 1992; Pollak et al, 1993]. As age
 711 increases by 4, heat fluxes decrease by 2, but in reality the decrease is very small. Today on average
 712 heat fluxes measured on the bottom surface through the ocean floor of the Miocene age (range 5.3-
 713 23.7 Myr) are equal to 81.9 mW/m², of the Oligocene age [23.7-36.6 Myr) to 62.3 mW/m² [Pollak et
 714 al., 1993]. On the oldest ocean floor (Late Jurassic, 144-163 Myr) the mean heat flux is relatively
 715 high, 51.3 mW/m² [Pollak et al., 1993].

716 In the first approximation, the heat flux through the old lithosphere is equal to the heat-
 717 conductivity coefficient of the lithosphere multiplied by the temperature gradient in the lithosphere,
 718 which in turn is equal to the change in temperature between the top and floor of the lithosphere,
 719 divided by its thickness. Consequently, to explain such high heat fluxes from the old ocean floor it is
 720 necessary to suppose very high solidus upper mantle temperatures of -1450°C (that is almost
 721 liquidus), and a very high coefficient of heat conductivity – 3.14 W/m°C [Khromov and Petrosyanc,
 722 2001]. Even at these high values, and with a lithosphere thickness of 95 km [Khromov and
 723 Petrosyanc, 2001], the heat flux will be only 48 mW/m² [Khromov and Petrosyanc, 2001].

724 However, using such parameters, heat fluxes calculated for the young oceanic lithosphere strongly
725 exceed heat fluxes measured on the ocean bottom [Stein and Stein, 1992; Pollak et al., 1993] – for
726 Miocene crust by 40 mW/m^2 and for Oligocene crust by 31 mW/m^2 [Pollak et al., 1993] – and
727 parameters of the model are significantly overstated. But if we subtract 40 mW/m^2 from these heat
728 fluxes related to warmer oceans in the LGM, then deep heat flux declines with motion from the rift
729 zone would be much higher: the Miocene crust would emit 41.9 mW/m^2 , and the late Jurassic crust
730 would emit 11.3 mW/m^2 – in four times. Same with the theory. If we take a more realistic value of
731 solidus hydrous peridotites – 950°C [Nobes et al., 1991] – and a coefficient of heat conductivity of
732 $1.5 \text{ W/m}^\circ\text{C}$ (remembering that heat conductivity tends to strongly decline as temperatures increase
733 [Schloessin and Drovak, 1977; Petrunin et al., 1971]), then for the same thickness of lithosphere we
734 would obtain a heat flux of 15 mW/m^2 , which is 3 times less. If we add 40 mW/m^2 to it then we
735 would obtain a heat flux through the ocean floor of 55 mW/m^2 . This is the most typical heat flux for
736 ocean bottom [Pollak et al., 1993].

737 Estimating average heat flux through the ocean floor, a value of 101 mW/m^2 was obtained
738 [Pollak et al., 1993]. At these heat flux calculations, fluxes through the young ocean crust (younger
739 than 66 million years) were calculated by a model [Stein and Stein, 1992]. This model, as we
740 showed, overestimated heat flux by ~ 3 times. On the rest of the territory, flux is overestimated by
741 40 mW/m^2 and possibly more, i.e by 3-4 times. As a result, average depth heat flux through ocean
742 crust does not exceed 35 mW/m^2 .

743

744 **3.2. Features of thermohaline circulation in the ocean**

745 Today, water in the ocean is stratified. The ocean interior is filled with cold and dense water,
746 while the surface layer is filled with warm, and therefore lighter, water. The ocean is unstratified
747 only in the high-latitude region, where both deep and surface waters are cold and dense. Such an

748 ocean can be mixed to its entire depth solely with winds. Let us assume that wind is pushing the
749 surface layer of water from the Northern Atlantic to the south, closer to the Antarctic. There, warm
750 water is cooled and becomes almost as dense as on the ocean floor. Even with minor force this water
751 can be submerged to the bottom. In the Northern Atlantic, water is transported south along the
752 surface, and in exchange, deep water is emerging. This motion does not require a large effort—both
753 on the surface and at depth, the water is similar in both temperature and density. As a result, under
754 pressure from a “wind pump”, water in the conveyor belt will circulate from the surface of one cold
755 sea to another.

756 Now let us investigate another hypothetical example: wind currents are absent, warm seas
757 with high salinity are absent, geothermal heat sources are absent, and all water in the ocean is mixed
758 and at a temperature of 20°C. In the mid- and high latitudes, water on the surface will cool and
759 become heavier than the interior water. Strong thermal convection will take place: cold and dense
760 water will submerge, and lighter, warmer water will emerge. The ocean will quickly cool and the
761 territory where convection takes place will shrink. When the ocean temperature declines to +5°C,
762 convection will take place only in the regions where surface water temperature is below +5°C. In
763 time, the ocean will cool below 0°C. On the ocean floor, only water from the freezing seas will
764 descend, and later only from the most cold and salty sea. As a result, the ocean will become filled
765 with the coldest and most dense water. After that, convection will basically stop. Everywhere on the
766 ocean, surface water will be lighter than water in the depth.

767 Now let us add to this scenario warm seas with high evaporation rates, with outflow of very
768 salty and dense water. Until all the ocean is warm and strong thermal convection takes place; these
769 small salty streams won't be noticeable. But with time the ocean will cool, thermal convection will
770 reduce, and these “haline” pumps will stop thermal convection. These seas absorb water with
771 normal salinity from the ocean surface and return (by precipitation) fresh water, transporting salt
772 down to the ocean interior. These seas desalinate the ocean surface. This reduces the density of the

773 water on the surface and consequently stops high-latitude convection. Only haline pumps will
774 continue working afterwards. They will strongly reduce salinity on the surface, and consequently
775 water entering these seas will be fresher, and outflow will also become less salty and less dense. At
776 some point, the haline pump will begin idling – outflow water will be lighter than interior ocean
777 water, and outflow will be spread in the lower parts of the ocean surface layer. In the end, only the
778 strongest haline pump will continue supplying water to the ocean bottom, but eventually it will stop.
779 Thermohaline circulation will stop.

780 Thermohaline circulation appears only under buoyancy forces, i.e. upwelling water must be
781 lighter than downwelling water. If their density becomes equal, motion forces will disappear and
782 convection will stop. Convection takes place either when the ocean is cooling or when there are heat
783 sources present at the bottom. Many researchers note that geothermal heat flow is important for
784 oceanic circulation [see refs. in Adkins et al., 2005]. We especially note that with no heating from
785 below, stable thermohaline circulation is impossible. The ocean water could be mixed by wind, but
786 this is not thermohaline circulation. Rayleigh's formula describes conditions for thermal convection.
787 In this formula, the thickness of the liquid layer is to a power of 3. For instance, in shallow lakes
788 convection appears at several degrees of temperature difference between the surface and the bottom,
789 whereas convection in the non-stratified ocean, which is 1000 times thicker, appears at a billion
790 times less temperature difference. An energy value of 50 mW/m^2 is tremendous, enough even for
791 convection to occur in the hard mantle. If all the energy converts into the kinetic energy of ocean
792 currents then all ocean water could reach a speed of 0.7 m/sec in one year.

793 Now let us add to our hypothetical scenario geothermal heat flux (unrealistically strong to
794 start with). First, an ocean at 20°C will cool, but then its temperature will stabilize: heat losses on
795 the surface will be compensated for by heat flux at the bottom. Convection will be very strong and
796 stable. If the geothermal heat flux is reduced, ocean temperature and thermal convection will also
797 reduce correspondingly. Reducing the geothermal heat flux, we can reduce the convection to the

798 point where the effect from haline pumps will become noticeable. At this point, they will quickly
799 desalinate the ocean surface. Later, they will start idling and ocean ventilation will stop, but heating
800 of the bottom waters will continue. Interior water temperatures will slowly increase. Water density
801 will decrease until it becomes lower than the density of the water flowing out of the strongest haline
802 pump. At this point, this pump starts working again. This pump will quickly reduce the surface
803 salinity and will start idling again. Then the ocean will warm up again, and so on.

804 Glaciers have a large influence on haline pumps. Expansion of glaciers leads to increased
805 salinity on the ocean surface and, consequently, increased salinity and density of water in haline
806 pumps. Therefore as long as ice accumulates haline pumps will rarely idle. Conversely, if glaciers
807 retreat, the surface salinity will decrease and haline pumps will idle until interior waters are heated.

808 Ocean heating cannot last forever. When at some point the density of water in the ocean
809 depths will become less than in the cold sea, then thermo pumps will turn on, salinity on the ocean
810 surface will immediately increase, and in cold seas very strong downwelling will occur (thus sharply
811 warming Arctic climate). It will continue until ocean would release all accumulated heat. However,
812 if there is a lot of ice on the surface of the cold sea and on surrounding land, then its quick melting
813 will decrease salinity and water density in cold seas; the thermo pump will stop and the release of
814 interior ocean heat will stop.

815 If, owing to tectonics or ocean regression, a strait which connects a haline sea with the ocean
816 becomes narrower and/or shallower, then regardless of ocean surface salinity, the salinity of down
817 flow from the haline pump will be high and decline in the salinity of the ocean surface will continue.
818 In an extreme case, a strait can become so shallow that outflow from it will stop and an evaporating
819 basin will occur. Salty water will still flow into the basin, and fresh water will return to the ocean
820 surface with precipitation. Such a basin of the same size as the Red or Mediterranean Seas can pump
821 out almost all the salt from the ocean surface, and the ocean will become ultra-stratified – water
822 exchange between the surface and the interior ocean would be very low owing only to diffusion.

823 Imagine an idealised extreme case: the ocean surface is totally desalinated, the density of the surface
824 water is close to 1000 kg/m^3 , the interior ocean water salinity is 35‰ and diffusion exchange of salt
825 and heat between the surface and the interior is absent. To take the ocean out of this stable state
826 would require heating the interior water up to 77°C . Only at that temperature would the density of
827 deep water drop to 1 g/cm^3 and convection would start.

828 In reality, as the ocean warms up, diffusion heat exchange with surface waters will increase
829 and become equal to deep heat flux, and after that ocean temperature rise will attenuate. A stable
830 state can then occur: fresh light water will lie above heavier but warmer water, i.e. because of
831 diffusive heat losses, bottom waters will not be able to heat to the point of overturning. With
832 diffusion, salt from the interior ocean will slowly penetrate to the surface. A salty sea will
833 continuously pump out this salt. This condition will be stable until the haline pump significantly
834 desalinates the entire ocean. Such a scenario likely did not occur in the Pleistocene, but it could have
835 occurred in other geological epochs when big evaporating basins were formed.

836

837 **4. Methods.**

838 **4.1. Mathematical model of thermohaline circulation**

839 To illustrate these features of thermohaline circulation and to reconstruct its dynamic in the
840 Pleistocene we present a simple 4-box model of the ocean. In this model we combine all cold seas
841 into one box with an area of $10.8 \cdot 10^6 \text{ km}^2$, which is eight times bigger than the area of the
842 Norwegian Sea. The thickness of the top, well-ventilated layer in this sea (in this box) and ocean (in
843 surface ocean box) is accepted to be 200 meters. The salty sea area is accepted to be $0.45 \cdot 10^6 \text{ km}^2$,
844 with an average depth of 550 meters. These values are the same as for the Red Sea. Thus we
845 consider a situation where there is only one haline pump against all thermo pumps.

846 The energy supplied from the sun and atmosphere is accepted to be $65 \cdot 10^8 \text{ J/m}^2/\text{yr}$ to the
847 high-latitude sea, $220 \cdot 10^8 \text{ J/m}^2/\text{yr}$ to the salty sea, and $130 \cdot 10^8 \text{ J/m}^2/\text{yr}$ to the box of the ocean

848 surface [Khromov and Petrosyanc, 2001]. The surface of each of these boxes emits energy into the
849 space, depending on the temperature of the water in this box, according to the Stefan-Boltzmann law
850 [Khromov and Petrosyanc, 2001]. Part of the energy in the salty sea is spent on the evaporation of
851 3.3 meters of water annually. This water and the energy of phase change are transported to the
852 surface of the open ocean box. The deep ocean box is receiving additional energy of 75 mW/m^2
853 from geothermal and biological heat flux.

854 We have accepted that the exchange of water between boxes is proportional to the difference
855 in water density in these boxes, i.e. in this scenario we are considering only thermohaline
856 circulation. The density of water in each box is calculated using a known formula based on salinity
857 and temperature. The coefficient of water exchange between the salty sea and the ocean surface is
858 accepted to be $0.003 \cdot 10^{15} \text{ m}^6/\text{kg} \cdot \text{yr}$. At this coefficient, salinity, temperature and water exchange in
859 this sea under the present conditions will be the same as in the Red Sea. As long as the water
860 density in these boxes is low, they exchange water only from the ocean surface box, but as soon as
861 their density becomes more than in the bottom reservoir, all water flowing out from the salty sea
862 drops down to the depths.

863 The coefficient of water exchange between the cold sea and the ocean surface box is
864 accepted to be equal to $0.15 \cdot 10^{15} \text{ m}^6/\text{kg} \cdot \text{yr}$. As soon as the water density in the cold sea becomes
865 higher than in the deep reservoir water starts to sink down. For this flow, we accept that the
866 coefficient is equal to $5 \cdot 10^{15} \text{ m}^6/\text{kg} \cdot \text{yr}$. These coefficients are selected so that the temperature in the
867 cold sea under the present conditions is close to 0°C and flux to the bottom is close to $0.6 \cdot 10^6$
868 km^3/yr ($\sim 20 \text{ Sv}$). At the appearance of flow from the cold sea to the bottom, additional
869 (compensative) flow appears from the ocean surface to the cold sea and from depth to the ocean
870 surface. If the density of water in the surface ocean box becomes more than that at the ocean bottom
871 then downwelling also occurs. For this water exchange we took the same coefficient as for the cold

872 sea. As soon as the water density in one of the surface boxes becomes less than the water density in
873 the bottom reservoir, downflows from this box stop.

874 All these currents redistribute salt and heat between boxes. As a result, for each box we have
875 budget equations for water, salt and heat. Visual description of the model is presented in the figure
876 4.

877 Now let us discuss the wind's role in ocean mixing. The role of the wind in the water
878 exchange in the Bab el Mandeb Strait can be neglected. Thermohaline circulation dominates there.
879 But in the water exchange between ocean surface and cold sea this is a valuable parameter. In the
880 first approximation, water exchange is proportional to wind strength, and wind strength is, in turn,
881 proportional to the meridional temperature gradient of the atmosphere, which in its turn depends on
882 the temperature difference between warm ocean and cold seas; i.e. we can accept this water
883 exchange as being proportional to the temperature difference between ocean and cold sea. We
884 accept that thermohaline circulation in these boxes is proportional to water density gradient.
885 However, water density in these boxes is proportional to water temperature (salinity in these boxes
886 is almost the same), so it appears that both wind and density mixing are proportional to temperature
887 difference. Both these dependencies can be united using a united coefficient of proportionality. We
888 can assume that the accepted above coefficient characterises both wind and density water exchange.
889 The density of water in the warm ocean is substantially lower than in the interior ocean; therefore
890 wind and diffusion exchange between these two boxes can be neglected. Wind exchange of water
891 can occur between the cold and interior boxes. In modern models, such water exchange is obtained
892 using accepted parameterization parameters. But in these seas heating from the bottom is not
893 accounted for. This heating can sustain the observed water exchange, and without wind. We have a
894 way to estimate the wind's role in the exchange with the bottom water. We know that the ocean
895 bottom in the LGM was warm. All heat flow measurements in the sediments on the ocean floor
896 show this. If wind exchange intensity were stronger than thermal convection, then haline pumps

897 would not be able to freshen the ocean surface and turn thermal pumps off. If low power sources
898 have managed to warm the ocean then wind couldn't stop it, and this means that wind exchange is
899 weaker than thermal convection.

900 In our scenario, we have added the ice accumulation into the equations for cold sea. As soon
901 as the average temperature of the cold sea drops below 0°C , fresh ice starts to accumulate both on
902 the surrounding land and in the sea. Salinity in this box consequently increases, and an additional
903 source of heat appears (80 calories per gram of frozen water). On the other hand, as soon as the
904 temperature of the water in this sea increases above 0°C , ice which has accumulated on the coast or
905 is floating in the sea melts, consuming energy and reducing salinity. We have accepted that ice
906 build-up and melting is proportional to the change between 0°C and the temperature of water in the
907 cold sea. Coefficients are such that a temperature change in the sea of -1°C in a thousand years
908 accumulates $4.86 \cdot 10^6 \text{ km}^3$ of ice. We have also accepted that the ice accumulation rate decreases
909 linearly as its volume increases (larger glaciers have greater deflation and ablation). We have
910 accepted a coefficient of proportionality such that the ice volume could not exceed a value
911 equivalent to a 150 m layer of ocean water. We have also accepted that area and depth of seas are
912 not influenced by change in ice volume, only by deep reservoir volume change.

913 The depth of Bab el Mandeb strait was changing with changing ice sheet dynamics.
914 However, in this scenario we have decided not to account for that. First of all, it was most important
915 for us to see whether the modern Red Sea can turn all thermal pumps off. Secondly, at a four-fold
916 decline in the cross section of this strait, because of increased salinity, water exchange there would
917 decrease only two-fold. Salinity will increase and therefore the power of this freshening pump will
918 not decline. The energy of this pump (the essence of its work) comes from the evaporation of 3.3
919 meters of water annually. This value is independent of the strait's cross section.

920 Saltier water is less compressible; thus it is harder to submerge it to the bottom. To describe
921 this thermobaric effect and model its short-period cyclicity [Adkins et al., 2005] we use a restricted

922 haline pump – water from this pump reaches a bottom reservoir only if its density is 0.25 kg/m^3
923 more than the current density in the bottom reservoir. Initial parameters are set at 25°C water
924 temperature and 34.7‰ salinity in all boxes.

925 The essence of our model is very simple. We have set box sizes close to real basins, we have
926 set external energy sources (in this model they are stable), and we have set coefficients of the water
927 exchange intensity. In reality these are the sizes of the openings connecting boxes – cross sections of
928 straights. Between salty sea and ocean, this strait (Bab el Mandeb)—this opening—is the smallest.
929 The strait between cold sea and the ocean is 50 times bigger (this is the width of the Northern
930 Atlantic), and the area of the opening between cold sea and underlying interior ocean is 33.3 times
931 more than that (depth of the “straight” is equal to ocean depth there), i.e. we have only set the
932 geometry of the system and external sources. The model calculates everything else: salinity,
933 temperature, density, water exchange. Water exchange between boxes is proportional to the density
934 difference between them.

935

936 **4.2. Model results**

937 The dynamic of modelled ocean parameters based on the solutions of the set of all budget
938 equations described above appears in Figure 5. We see that our model ocean has lost all initial heat
939 in 16,000 years. Temperature in the depth decreased from 25°C to 1.6°C . At that point a noticeable
940 decline in the salinity of surface waters was observed, and the haline pump quickly turned off
941 thermal circulation – a glacial period had started. During glaciation, the haline pump was often
942 idling and worked permanently only at the end of the glaciation period. The duration of the glacial
943 period was 112,000 years, the same as the Pleistocene glacial periods. For the duration of the glacial
944 period, ice accumulation in seas and on land was equivalent to 149.5 meters of water in the world
945 ocean. The salinity on the ocean surface declined to 31‰ and on the sea bottom increased to
946 36.5‰ . These correspond to estimations made for the LGM. The average temperature of water in

947 the deep reservoir increased to 23.4° C and water density dropped to 1,024.9 kg/m³ and became the
948 same as in the cold sea. After that, active downwelling appeared in the cold sea. Owing to the sea
949 strong warming, all ice quickly melted. During several hundred years, there were no winters on the
950 coastal areas of the seas. In 14,600 years, the ocean has again lost all accumulated heat and a new
951 glaciation period has started. We found that the duration of the interglacial was the same as the age
952 of the sharp warming in Greenland in Boling-Alerd 14,650 years ago. Our model has shown a
953 temperature of 1.6°C on the ocean bottom at the end of the interglacial period. This is the present
954 ocean temperature.

955 We see that the simple model of thermohaline circulation under stable external conditions
956 shows asymmetric cycles which look like glacial cycles. We did not try to make a super-precise
957 model; all initial parameters are rounded values. However the duration and amplitude of both glacial
958 cycles correspond with observed values. The model even indicates a short cooling somewhat similar
959 to the Younger Dryas and also short-term cycles similar to Dansgaard/Oeschger warm events.

960 To test the model, we have substantially changed initial parameters and increased the number
961 of boxes in the model, but if the depth heat flux is small and if the “pressure” of haline pumps is
962 stronger than that of cold pumps then in all cases we obtain ocean heating. Glacial cycles get shorter
963 if bottom heating is increased. If the haline pump is further restricted, this causes occasional turning
964 on of the cold pump and Dansgaard/Oeschger warm events appear [Adkins et al., 2005]. If we
965 remove glaciers from the model, the haline pump is often idling and glacial cycles are longer. But if
966 deep heat flux were removed, then thermal circulation in the ocean would stop, and soon haline
967 pumps would idle and thermohaline circulation would stop forever.

968 For the “Northern Atlantic” we have obtained a very strong temperature dynamic, but for the
969 rest of the ocean the temperature dynamic on the surface does not exceed 1°C (see figure 1). But if
970 were to add the Earth’s orbit dynamic, decline in greenhouse gas concentration in the atmosphere,

971 albedo change related to forest area decrease, and increase of snow and ice covered territories, then
972 ocean surface cooling in the glaciation period would be substantially stronger.

973 Here we want to note that if a more detailed model were to be developed, it should take into
974 account that the main ocean heating from the bottom occurs in the rift zones, on depths of 2–3 km,
975 and big masses of water penetrating from the Red Sea at the beginning of glaciation would be
976 cooling, heating up the cold floor.

977 The main proof of ocean warming in the last glaciation period is the high remaining heat flux
978 from the sediments of the ocean floor. Our model has shown the mechanisms and dynamics of this
979 warming. Close correlation between observed values and modelling results is an additional proof for
980 ocean warming.

981

982 **5. Discussion.**

983 **5.1. Consequences of warm ocean hypothesis**

984 Many of the views on natural processes in the Pleistocene are coordinated with the cold
985 ocean hypothesis. Rejecting this hypothesis requires a revision of these views.

986 Today, air temperature at the North Pole in summer is close to 0°C. At that time, ice melts
987 there. The Arctic receives lots of heat from the Atlantic. Therefore ice cover in the Arctic Ocean is
988 thin and firm. Ocean currents and wind break this cover and transport ice south. If the temperature in
989 Greenland in the LGM was 25°C colder than it is today [Dahl-Jensen, 1998], and if the heat
990 conveyor did not work, then ocean ice cover would have been thicker and would never have melted
991 [Bradley and England, 2008]. Sea water freezing becomes slower as ice thickness grows. But the
992 surface of Arctic ice receives precipitation of, on average, ~10 cm of water in the form of snow.
993 During the glaciations, when the Arctic was substantially colder, this snow never melted. The areas
994 of the Antarctic and Arctic Oceans are comparable. The amounts of snow precipitating on these
995 areas are also comparable. In the Antarctic, the thicker the ice sheet the faster is its motion. Antarctic

996 ice flows to the ocean through a “strait” almost 20,000 kilometers wide. In the Arctic Ocean, the
997 situation is opposite: ice flows south through narrow and shallow straits. The thicker and harder is
998 the ice in the Arctic, the harder it is for winds and currents to press it through these straits. In the
999 glaciation period, these straights were even shallower. The smaller the ice outflow, the more
1000 intensively it accumulates in the Arctic. At such dependency, spontaneous and irreversible
1001 glaciation of the entire Arctic Ocean is possible. There must have been floating sea glaciers with
1002 very low ice $\delta^{18}\text{O}$. These glaciers would have been mostly submerged, with only 9% of their volume
1003 above the water surface, i.e. only 90 m of a 1 km deep glacier would be above sea level. Such a
1004 glacier could not flow into land or penetrate to the Atlantic through shallow straits. A 1 km iceberg
1005 could not go through a 100 m depth strait. At an ice accumulation rate of 10 cm/yr, the Arctic Ocean
1006 could be filled three times over with free-saline ice during glacial periods. If this glacier hit the
1007 bottom of the ocean somewhere, then it should start growing rapidly above water level in this place.
1008 This would result in the ice flowing.

1009 In the global budget of $\delta^{18}\text{O}$, made in the framework of the cold ocean theory, there is no
1010 place for such a big floating reservoir of isotopically light ice. However in the framework of the
1011 warm ocean, the appearance of such a reservoir is very likely.

1012 During the last glaciation, $\delta^{13}\text{C}$ in the ocean water declined by 0.3–0.4‰. It is assumed that
1013 the reason for this was that the terrestrial reservoir of organic carbon decreased by 500 Pg C,
1014 because of forest areas shrinking, and this isotopically light carbon was absorbed by the ocean
1015 [Sigman and Boyle, 2000]. The methane content in depth sediments is 10000–20000 Pg [Kennet et
1016 al., 2000]. Today it is stable; layers of solid gas clathrates prevent underlying methane from
1017 escaping. But if water temperature on the ocean bottom has changed significantly, then most of the
1018 gas clathrates of the World Ocean melted during glacial periods. Water level and pressure were
1019 lower, and this accompanied the emission of hundreds of pentagrams of methane from bottom
1020 sediments, dissolution of methane in the water, and further oxidation to CO_2 . $\delta^{13}\text{C}$ of gas clathrates

1021 is very low (-65‰) [Kennet et al., 2000], therefore $\delta^{13}\text{C}$ of ocean water was reduced during
1022 glaciations. An emission of 170 Pg C equivalent of this methane (this is only 1–2% of global storage
1023 of the methane on the ocean bottom) will have the same effect on $\delta^{13}\text{C}$ of oceanic water as an
1024 emission of 500 Pg C from terrestrial or oceanic organic reservoirs.

1025 At low circulation in glacial periods, oxygen input to the bottom decreased, but at the same
1026 time nutrition supply to the surface from the depth also declined by the same level of magnitude and
1027 consequently the biological pump was reduced as well, i.e. oxygen input was lower but its
1028 consumption was low as well. Therefore there were few anoxic conditions on the ocean floor.
1029 Additionally, bottom water was heated by geothermal and biological heat, therefore despite low
1030 content of dissolved gases, their partial pressure was increasing. If such warm gas-saturated water
1031 eventually emerged on the ocean surface, it would first emit gases into the atmosphere, and only
1032 after cooling would it strongly absorb them.

1033 During the glaciation period CO_2 concentration in the atmosphere declined; it lost ~200 Pg of
1034 carbon. Carbon content in forests was reduced by 500 Pg. It is thought that this carbon was absorbed
1035 by the ocean and then in deglacial periods it was returned to the atmosphere and to the land [Sigman
1036 and Boyle, 2000]. However, mechanisms for this are still unclear [Sigman and Boyle, 2000; Kohfeld
1037 et al., 2005]. On the contrary, there are several data sets which give evidence of decreased carbon
1038 storage in the glacial ocean: i) Storage of organic carbon in the ocean is comparable in size with the
1039 terrestrial organic carbon reservoir (their $\delta^{13}\text{C}$ signatures is the same) [Brovkin et al., 2002]. Ocean
1040 productivity in the glacial period decreased significantly [Kohfeld et al., 2005; Anderson et al.,
1041 2009; Zimov et al., 2009]. Only at the end of glaciation, when the ocean had substantially heated
1042 and circulation had slightly increased (see Fig. 1), did productivity increase in the Atlantic [Kohfeld
1043 et al., 2005; Zimov et al., 2009]. Therefore the dissolved organic carbon content of the ocean's water
1044 and carbon storage at the bottom should be correspondingly lower; ii) The salinity of the glacial
1045 ocean increased (because of glacier growth), and its CO_2 solubility capacity decreased

1046 correspondingly [Sigman and Boyle, 2000]; iii) An attempt to find proof of 700 Pg deglaciation
1047 emission from the ocean to the atmosphere was made by Yu et al. [2010]. The data indicated that the
1048 carbonate ion concentration of the deep ocean during deglaciation increased only by 10 mmol/kg,
1049 and only in the deepest part of ocean [Yu et al., 2010]. It is equal to a 100 Pg C loss from the deep
1050 reservoir [Yu et al., 2010]. In the other 70% of the ocean volume the carbonate ion concentration
1051 strongly decreased during deglaciation [Yu et al., 2010; Zeebe and Marchitto, 2010] (by 60 mmol/kg
1052 at the ocean's surface [Yu et al., 2010]). If all these data are interpolated, then the carbonate ion
1053 content of the entire ocean decreased by 20–25 mmol/kg and the ocean absorbed as little as 700 Pg
1054 inorganic carbon during deglaciation.

1055 CO_2 dissolution in water is strongly dependent on water temperature. Therefore carbon
1056 storage in the ocean can be increased by cooling of the ocean [Sigman and Boyle, 2000]. However,
1057 the possibilities of this explanation are limited, as today the interior ocean temperature is close to the
1058 point of freezing. Therefore only one third of atmospheric CO_2 decline in glaciation can be
1059 explained by slight cooling (2–3°C) of the ocean [Sigman and Boyle, 2000]. But all deep boreholes
1060 show strong ocean warming. The ocean was half-filled with warm (much CO_2 depleted) water from
1061 the Red Sea, and the carbon content of ocean water during the glaciations must have been very
1062 strongly reduced because of that. Accounting for all of the above, carbon storage in the LGM ocean
1063 was reduced by approximately 1,500 Pg C. That means that there should be some other big carbon
1064 reservoir which greatly increased in size during the glaciation period and absorbed carbon from the
1065 atmosphere, forest ecosystems, gas clathrates, and ocean carbon reservoirs. Of all known carbon
1066 reservoirs, only permafrost and soils of the mammoth steppe biome could absorb such amounts of
1067 carbon. In the LGM, resting on the permafrost mammoth steppe was the earth's biggest biome. It
1068 was a highly productive ecosystem, where hundreds of millions of large herbivores maintained their
1069 pastures [Zimov et al., 2012]. Only soils of the cold biome are capable of accumulating hundreds of
1070 kilogram's of carbon per square meter [Zimov et al., 2006; Zimov et al., 2009]. Today, permafrost is

1071 the largest reservoir of organic carbon (1670 Pg C [Tarnocai et al., 2009]), and in the LGM it was at
1072 least twice as big. The mammoth steppe biome pumped light carbon from other reservoirs into its
1073 frozen soils.

1074 During the Pleistocene-Holocene transition increased not only atmospheric CO₂
1075 concentration, but also concentration of the atmospheric methane. An analysis of global ¹⁴C data for
1076 basal peat combined with modelling of wetland succession allowed us to reconstruct the dynamics
1077 of global wetland methane emission through time. These data show that the rise of atmospheric
1078 methane concentrations during the Pleistocene-Holocene transition was not connected with wetland
1079 expansion, but rather started substantially later, only 9 thousand years ago. [Zimov and Zimov
1080 2014]. The isotopic composition of methane varies according to source. Owing to ice sheet drilling
1081 programs past dynamics of atmospheric methane isotopic composition is now known. Modelling of
1082 the budget of the atmospheric methane and its isotopic composition allowed us to reconstruct the
1083 dynamics of all main methane sources. For the late Pleistocene, the largest methane source was
1084 megaherbivores, whose total biomass is estimated to have exceeded that of present-day humans and
1085 domestic animals. During deglaciation, the largest methane emissions originated from degrading
1086 frozen soils of the mammoth steppe biome. Methane from this source is unique, as it is depleted of
1087 all isotopes. We estimated that over the entire course of deglaciation (15,000 to 6,000 year before
1088 present), soils of the mammoth steppe released 300–550 Pg (10¹⁵ g) of methane. This is
1089 approximately 300 Pg C [Zimov, Zimov 2014].

1090 What was the total carbon loss from the northern soils over that time period? Even in fully
1091 anaerobic conditions only part of the stored organic (28±12%) can be transformed into methane
1092 [Walter Anthony et al. 2014]. When thick (tens of meters) frozen ice-rich soils (yedoma and its
1093 southern analogues) thaw they are initially anaerobic, however, as permafrost degradation continues,
1094 underlying gravel and sand thaws and water begins to drain from shallower soil layers. These soils

1095 become aerobic and carbon is transformed into the CO₂. However on most territories occupied by
1096 the mammoth steppe, soils (both including active layer and soils incorporated into the permafrost)
1097 were shallow (less than 2–3 meters deep), and carbon stored in these soils was mostly decomposed
1098 under aerobic conditions when the climate warmed. Therefore, if we accept that 15% of permafrost
1099 carbon loss was transformed into methane, we can estimate that permafrost soils lost 2000 Pg C
1100 during deglaciation (15–6 ka BP) [Zimov and Zimov 2014]. This carbon is sufficient to supply
1101 Holocene forest expansion and fill the cooling ocean with CO₂.

1102 At present, the ocean has already released most of the accumulated heat from the last
1103 glaciation. Bottom sediments have also cooled, so thermo circulation has decreased. Soon it can be
1104 expected that salty seas will stop thermo circulation and a new glacial period will start (see Fig. 1).

1105 By artificially regulating water exchange in narrow straits which connect salty seas with the
1106 ocean, we may have the capacity to change the salinity and density of outflowing water. By
1107 increasing water exchange we might stop the freshening of surface water and may prolong the life of
1108 cold pumps. In contrast, if we could reduce the water exchange, the thermo circulation might slow
1109 more quickly and hasten the beginning of the next glacial cycle. This, to some extent, can
1110 compensate for warming caused by increased greenhouse gas concentrations in the atmosphere.

1111 However, the results of this experiment are doubtful. Today, the ocean absorbs half of all
1112 anthropogenic emissions of CO₂. But if thermo circulation is replaced by haline circulation, then the
1113 ocean interior will start warming and releasing CO₂ in addition to anthropogenic emissions. In the
1114 past, this emission was totally compensated for by permafrost and mammoth steppe expansion, but
1115 with the anthropogenic rise in atmospheric CO₂ concentrations, new permafrost will not be formed,
1116 and northern steppes will not expand in Europe. As a result, by changing thermo circulation to
1117 haline circulation we would double the rate of emissions of atmospheric CO₂ and see a strong
1118 decline in ocean productivity.

1119

1120 **6. Conclusions**

1121 Forty years ago, cold and warm ocean hypotheses were equal in rights – both were discussed.
1122 Neither one of them had enough proof. During that period of time the geology revolution started –
1123 the theory of plate tectonics was evolving, and it was very important to know why bottom sediment
1124 emits energy: either it is a mantle heat flow or these are bottom sediments releasing the heat
1125 accumulated during the last ocean warming. Temperature profiles from deep boreholes answer this
1126 question simply and reliably – if heat flux is stable with depth, then the first hypothesis is correct; if
1127 it declines, then the second hypothesis is correct. Oceans are connected with each other, therefore
1128 hypotheses are alternative: heat fluxes in the ocean bottom sediments should be either stable
1129 everywhere or decline everywhere. Therefore it is enough to reliably measure temperature in a few
1130 boreholes to choose the correct hypothesis.

1131 First three profiles of heat flux in ocean sediments were obtained in boreholes 184,185 and
1132 206. These are deep boreholes, and they have indicated a strong decline in heat flux with depth.
1133 Solely because of that, these data were excluded from previous analyses. All consequent deep
1134 boreholes indicated the same results and they were either also excluded from analyses or, contrary to
1135 the facts, it was stated that heat fluxes in these boreholes are stable and they prove the cold ocean
1136 hypothesis.

1137 One of the reasons why data from deep boreholes were not trusted was that they indicated
1138 extremely strong ocean warming in the LGM. It wasn't clear what the source for that ocean heating
1139 was. However, such sources exist, and they are sufficient for ocean warming. The heavy waters
1140 from the Red Sea, geothermal heat flux and decomposition of organic matter on the ocean floor.
1141 Flux of salty water to the ocean bottom from the Red Sea maintained freshening of the ocean surface
1142 and strong ocean stratification. In the absence of ocean mixing, even weak energy sources can warm
1143 the ocean interior. Strong stratification of water in the LGM is supported by data on salinity of the

1144 ocean on the surface and at the bottom, and data on low bioproductivity. The idea that the ocean in
1145 the glaciation was filled with Red Sea waters is supported by data on similar isotopic content of
1146 water in this sea and ocean bottom water in the LGM.

1147 We have made a mathematical model of thermo-haline circulation of the world ocean. We
1148 have taken sun energy income to the ocean surface, high-latitude seas and the Red Sea as constant
1149 and the same as today. Geothermal and biogenic bottom water heating we also took as constant. But
1150 as a result we obtained strongly asymmetrical glacial-interglacial cycles of ocean dynamic, climate
1151 and glaciers. The model showed that during the glacial period ventilation of the ocean sharply
1152 diminished. Thermal pumps didn't work, high-latitude seas froze. Warm and heavy water from the
1153 Red Sea filled all interior oceans. In 112,000 years, the salinity of surface waters has declined to
1154 31‰ (on the bottom it reached 36.5‰), and the average temperature of water in the interior ocean
1155 box reached 23.4° C. At that, its density has become lower than the density of water in high-latitude
1156 seas, which caused the start of very strong convection. As a result, in 14,600 years, the ocean has
1157 fully released all heat accumulated in the glacial period, and cooled to 1.6° C. Thermal pumps have,
1158 at that, slowed down, and haline pumps, at that, quickly decreased the salinity and fully stopped the
1159 thermal circulation. Ocean interior warming has started anew – a new glacial cycle has started anew.
1160 The cyclicity obtained in the model is very close to observed glacial-interglacial cycles, both by the
1161 amplitude and by the duration.

1162 The uniqueness of the variable Pleistocene climate is likely connected with the fact that very
1163 cold and very salty seas and frozen soils, which could accumulate large amounts of carbon, appeared
1164 on our planet at the same time. From the analyses presented it follows that during glaciation epochs,
1165 haline circulation dominated – the ocean was taking up warm water from the surface and
1166 accumulating heat. On land, polar oceans and permafrost were accumulating ice and ocean bottom
1167 “ice” (gas clathrates) was melting. Interglacials are epochs when the ocean is dominated by thermo
1168 circulation – the ocean absorbs the coldest water and releases its heat. In the ocean bottom, water

1169 and methane crystallise while on the land, glaciers and permafrost thaw. Microbes turn into CO₂ and
 1170 CH₄, the organic which is accumulated in the permafrost and cold soils.

1171 Glaciations are periods when the ocean accumulated energy, and interglacials are periods when
 1172 the ocean quickly released this energy.

1173

1174 **References**

- 1175 1. Adkins, J.F., McIntyre, K., and D.P. Schrag (2002), The salinity, temperature and $\delta^{18}\text{O}$ of the
 1176 glacial deep ocean. *Science*, 298: 1769.
- 1177 2. Adkins, J.F., Ingersoll, A., and C. Pasquero (2005), Rapid climate change and conditional
 1178 instability of the glacial deep ocean from the thermobaric effect and geothermal heating.
 1179 *Quat Sci Rev*, 24: 581.
- 1180 3. Anderson, R.F., Ali, S., Bradtmiller, L.I., Nielsen, S.H.H., Fleisher, M.Q., et al. (2009),
 1181 Wind-Driven Upwelling in the Southern Ocean and the Deglacial Rise in Atmospheric CO₂.
 1182 *Science* 323: 1443.
- 1183 4. Badawi, A., Schmiedl, G., and C. Hemleben (2005), Impact of late Quaternary
 1184 environmental changes on deep-sea benthic foraminiferal faunas of the Red Sea. *Marine*
 1185 *Micropaleontology* 58: 13-30.
- 1186 5. Bradley, R.S., and J.H England (2008), The Younger Dryas and the sea of ancient ice. *Quat*
 1187 *Res* 70, 1.
- 1188 6. Brovkin, V., Hofmann, M., Bendtsen, J., and A. Ganopolski (2002), Ocean biology could
 1189 control atmospheric $\delta^{13}\text{C}$ during glacial-interglacial cycle. *GGG* 3,
 1190 10.1029/2001GC000270.
- 1191 7. Bryan, S.P., and T.M. Marchitto (2008), The Mg/Ca - temperature proxy in benthic
 1192 foraminifera: New calibrations from the Florida Straits and a hypothesis regarding Mg/Li,
 1193 *Paleoceanography*, 23: 1553.

- 1194 8. Chapin, III F.S., Matson, P.A., and H.A. Mooney (2002), Principles of terrestrial ecosystem
1195 ecology. Springer-Verlag, New York.
- 1196 9. Chuprynin, V.I. (1985), Interrupted autooscillation of geophysical systems. Nauka,
1197 Moscow,. (in Russian)
- 1198 10. Cuffey, K.M., Clow, G.D., Alley, R.B., Stuiver, M., Waddington, E.D., and R.W. Saltus
1199 (1995), Large Arctic Temperature Change at the Wisconsin-Holocene Glacial Transition.
1200 Science 270: 455.
- 1201 11. Dahl-Jensen, D., Mosegaard, K., Gundestrup, N., Clow, G.D., Johnsen, S.J., et al. (1998),
1202 Past Temperatures Directly from the Greenland Ice Sheet. Science 282: 268.
- 1203 12. de Vernal, A., and C. Hillaire-Marcel (2000), Sea-ice cover, sea-surface salinity and halo-
1204 /thermocline structure of the northwest North Atlantic: modern versus full glacial conditions.
1205 Quat Sci Rev 19: 65.
- 1206 13. Erickson, A.J., Von Herzen, R.P., Sclater, J.G., Girdler, R.W., Marshall, B.V., et al. (1975),
1207 Geothermal measurements in deep-sea drill holes. J Geophys Res 80: 2515–2528.
- 1208 14. Foucher, J.P., Chenet, P.Y., Montadert, L., and J.M. Roux (1984), Geothermal measurements
1209 during Deep Sea Drilling Project leg 80. Initial Rep. Deep Sea Drill. Proj. 80: 423.
- 1210 15. Geiselhart, S. (1998), Late Quaternary Paleoceanographic and paleoclimatic history of the
1211 Red Sea during the last 380,000 years: evidence from stable isotopes and faunal
1212 assemblages. Tüb Micropälaontol Mitt 17, 1.
- 1213 16. Hay, W. (1983), The global significance of regional Mediterranean
1214 Neogenepaleoenvironmental studies. In: Meulenkamp JE editor. Bull. 30 Reconstruction of
1215 marine paleoenvironments. Loonzetterij Abe, Hoogeveen Netherlands.
- 1216 17. Hemleben, C., Meischner, D., Zahn, R., Almogi-Labin, A., Erlenkeuser, H., et al. (1996),
1217 Three hundred eighty thousand year long stable isotope and faunal records from the Red Sea:
1218 Influence of global sea level change on hydrography. Paleoceanography 11: 147-156.

- 1219 18. Hyndman, R.D., Langseth, M.G., and R.P. Von Herzen (1987), Deep Sea Drilling Project
1220 geothermal measurements: A review. *Rev of Geophys* 25, 8: 1563.
- 1221 19. Kennett, J.P., Cannariato, K.G., Hendy, I.L., and R.J. Behl (2000), Carbon isotopic evidence
1222 for methane hydrate instability during quaternary interstadials. *Science* 288: 128.
- 1223 20. Khromov, S.P., and M.A. Petrosyanc (2001), *Meteorology and Climatology*. Moscow
1224 University Press, Moscow.
- 1225 21. Kohfeld, K.E., Le Quéré, C., Harrison, S.P., and R.F. Anderson (2005), Role of marine
1226 biology in glacial-interglacial CO₂ cycles. *Science* 308: 74.
- 1227 22. Luz, B., and Z. Reiss (1983), Stable carbon isotopes in Quaternary foraminifera from the
1228 Gulf of Aqaba (Elat), Red Sea. In: Meulenkamp JE editor. *Bull. 30 Reconstruction of marine*
1229 *paleoenvironments*. Loonzetterij Abe, Hoogeveen, Netherlands.
- 1230 23. Miles, P.R. (1995), Potential distribution of methane hydrate beneath the European continental
1231 margins. *Geophys Res Lett* 22: 3179.
- 1232 24. Nobes, D.C., Mienert, J., Mwenifumbo, C.J., and J.P. Blangy (1991), An estimate of the heat flow on
1233 the meteor rise, site 704. *Proceedings of the Ocean Drilling Program, Scientific Results*, 114: 39.
- 1234 25. Petrunin, G.I., Yurchak, R.I., and G.F. Tkach (1971), Temperature conductivity of Basalts at
1235 temperatures from 300 to 1200°K. *Izv: Earth Phys*, 2: 65. (In Russian)
- 1236 26. Pollak, H.N., Hurter, S.J., and J.R. Johnson (1993), Heat flow from the Earth's interior: Analysis
1237 of the global data set. *Rev of Geophys* 31: 267.
- 1238 27. Sarnthein, M. (2011), Paleoclimate. Northern meltwater pulses, CO₂, and changes in
1239 Atlantic convection. *Science* 331: 156.
- 1240 28. Schloessin, H.H., and Z.D. Drovak (1977), Physical properties of samples from the joides, leg 36,
1241 Deep Sea Drilling Project. *Initial Rep Deep Sea Drill Proj* 37: 403.
- 1242 29. Severinghaus, J.P., and E.J. Brook (1999), Abrupt climate change at the end of the last glacial
1243 period inferred from trapped air in polar ice. *Science* 286: 930, 1999.

- 1244 30. Sigman, D.M., and E.A. Boyle (2000), Glacial/interglacial variations in atmospheric carbon
1245 dioxide. *Nature* 407: 859.
- 1246 31. Stein, C.A., and S. Stein (1992), A model for the global variation in oceanic depth and heat
1247 flow with lithospheric age. *Nature* 359: 123.
- 1248 32. Tarnocai, C., Canadell, J.G., Schuur, E.A.G., Kuhry, P., Mazhitova, G., and S. Zimov
1249 (2009), Soil organic carbon pools in the northern circumpolar permafrost region. *Global*
1250 *Biogeochem Cycles* 23: 2023.
- 1251 33. Van der Zwaan, G.J., Duijnste, I.A.P., Den Dulk, M., Ernst, S.R., Jannink, N.T., et al.
1252 (1999), Benthic foraminifers: proxies or problems? A review of paleocological concepts.
1253 *Earth Sci Rev* 46: 213–236.
- 1254 34. Walter Anthony K.M., Zimov S.A., Grosse G., Jones M.C., Anthony P, et al. (2014),
1255 Permafrost thaw by deep lakes: from a methane source to a Holocene carbon sink. *Nature*,
1256 Submitted.
- 1257 35. Washburn, A.L. (1979), *Geocryology, A survey of periglacial processes and environments*.
1258 Edward Arnold, London.
- 1259 36. Yershov, E.D. (2004), *General Geocryology*. Cambridge University Press.
- 1260 37. Yu, J., and H. Elderfield (2008), Mg/Ca in the benthic foraminifera *Cibicidoides*
1261 *wuellerstorfi* and *Cibicidoides mundulus*: Temperature versus carbonate ion saturation. *Earth*
1262 *and Planet Sci Lett* 276: 129.
- 1263 38. Yu, J., Broecker, W.S., Elderfield, H., Jin, Z., McManus, J., and F. Zhang (2010), Loss of
1264 carbon from the deep sea since the Last Glacial Maximum. *Science* 330: 1084.
- 1265 39. Zeebe, R.E., and T.M. Marchitto, Jr. (2010), Atmosphere and ocean chemistry. *Nature*
1266 *Geoscience* 3: 386.
- 1267 40. Zimov, N.S., Zimov, S.A., Zimova, A.E., Zimova, G.M., Chuprynin, V.I., and F.S. III
1268 Chapin (2009), Carbon storage in permafrost and soils of the mammoth tundra-steppe biome:

- 1269 role in the global carbon budget. *Geophys Res Lett* 36, L02502,
 1270 doi:10.1029/2008GL036332.
- 1271 41. Zimov S.A., and N.S. Zimov (2014), Role of Megafauna and Frozen Soil in the Atmospheric
 1272 CH₄ Dynamics. *PLoS ONE* 9(4): e93331. doi:10.1371/journal.pone.0093331.
- 1273 42. Zimov, S.A., Zimov, N.S., Tikhonov, A.N., and F.S. III Chapin (2012), Mammoth steppe: a
 1274 high-productivity phenomenon. *Quat Sci Rev* 57: 26-45.
- 1275 43. Zimov, S.A., Schuur, E.A.G., and F.S. III Chapin (2006), Permafrost and the global carbon
 1276 budget. *Science* 312: 1612.

1277
 1278

1279 **Figure captions**

1280 **Figure 1.** Profile of bottom sediment temperatures and profile of conductive heat flows for
 1281 scenarios of cycling changes of ocean bottom temperatures from +2⁰C to +32⁰C during glacial-
 1282 interglacial dynamic. The red lines are temperature profiles for various deep heat flows at the time
 1283 of maximum heating of the ocean floor. The green and blue lines are temperature and heat flow
 1284 profiles for the time periods of 11470 years and 14450 years after sharp ocean cooling. A –scenario
 1285 for sediments not saturated with methane. B –scenario showing gas hydrate formation. Knees on the
 1286 temperature profiles and leaps on heat flow profiles show gas hydrate bottom. C – temperatures and
 1287 heat flows at stable temperature on the bottom (+2⁰C) and at the same deep heat flows.

1288

1289 **Figure 2.** Profiles of temperatures, thermal conductivity, temperature gradients and heat flow
 1290 in the bottom sediments in the open ocean.

1291 A – boreholes measured during legs 1-26 and available in the review [Erickson et al., 1975].
 1292 Data marked with orange columns were taken from the resultant graph [Erickson et al., 1975]. The
 1293 blue arrows are our data corrections. B – all deep boreholes measured during DSDP and noted in the

1294 review (Hyndman et al., 1987). C – deep boreholes measured during ODP and IODP. Thermal
1295 conductivity data: large dots – are average values for depth intervals as shown in the initial reports;
1296 small dots are initial values; circles are average values of thermal conductivity per depth intervals
1297 that we calculated from initial data. The numerals on the figures are number of leg, number of
1298 borehole and ocean depth. The blue dotted lines are the depth where gas hydrates freeze or thaw
1299 [Miles, 1995]. If sediment temperature lies to the left of this line, then at high methane concentration
1300 it will be in the form of gas clathrates. To the right of this line gas clathrates are absent. All
1301 boreholes in the figure show a strong decrease of heat flux with depth. This means strong heating of
1302 the ocean in the LGM. Only borehole 1352 (depth 344 m) shows an increase in heat flow with
1303 depth. This states that on the New Zealand shelf water in the LGM was colder than today.

1304 **Figure 3.** Map of boreholes noted in the Figure 2.

1305 **Figure 4.** Ocean circulation scheme for glacial and interglacial used in presented model.

1306 **Figure 5.** Results of model of thermo-haline circulation in the World Ocean. Red line – Red
1307 sea; Blue line – high latitude seas; Green line – Ocean surface; Black line – Ocean interior.

1308

1309

1310

1311

1312

1313

1314

1315

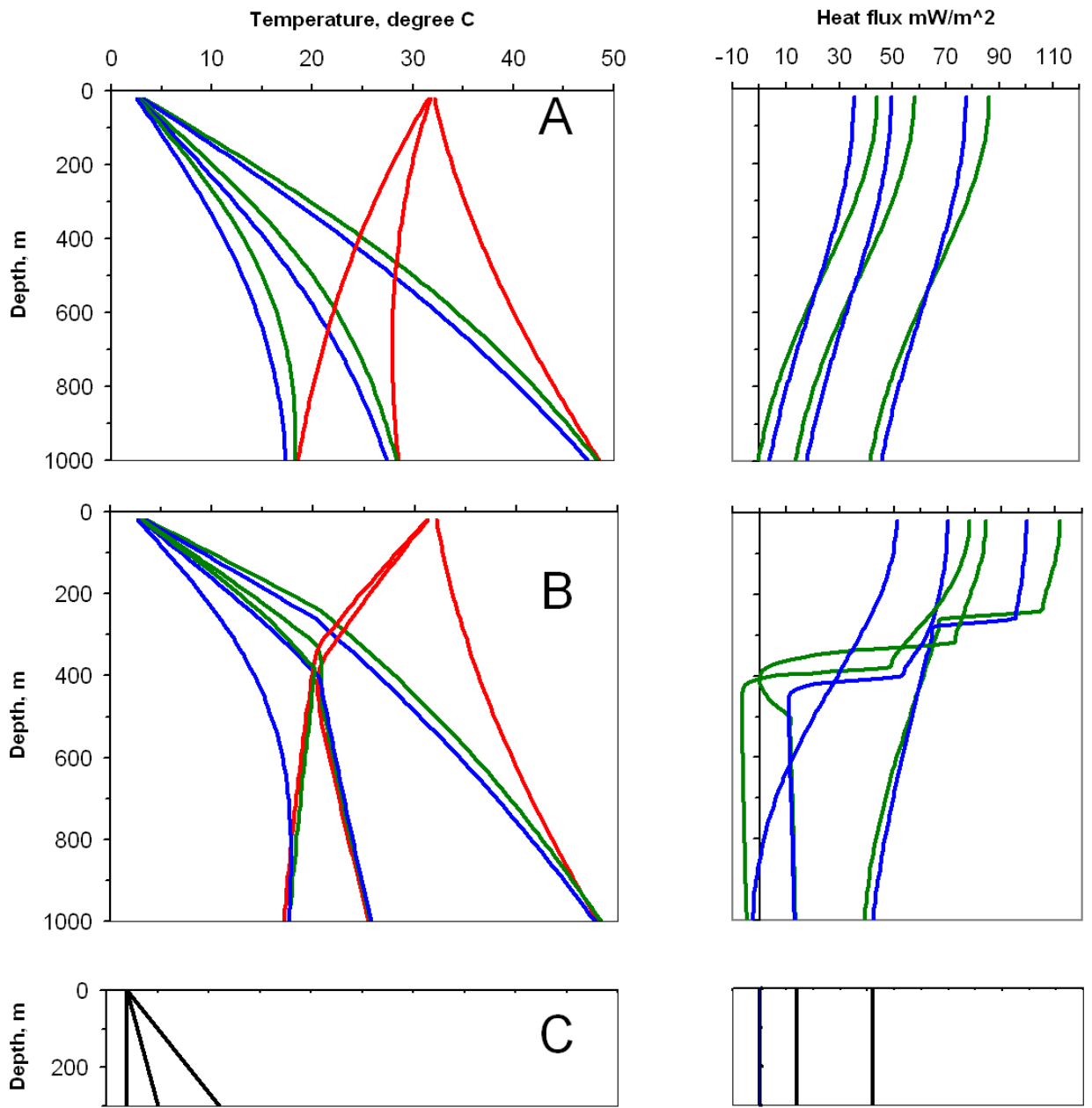
1316

1317

1318

1319

Fig. 1



1320

1321

1322

1323

1324

1325

1326

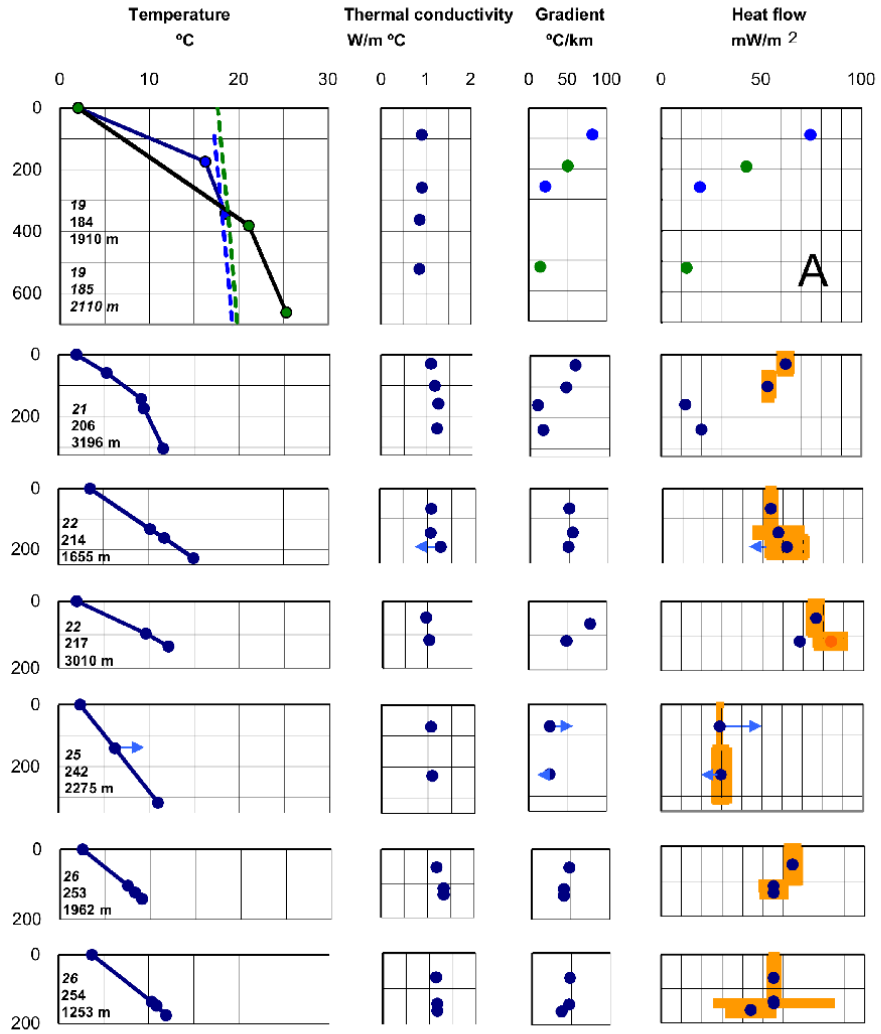
1327

1328

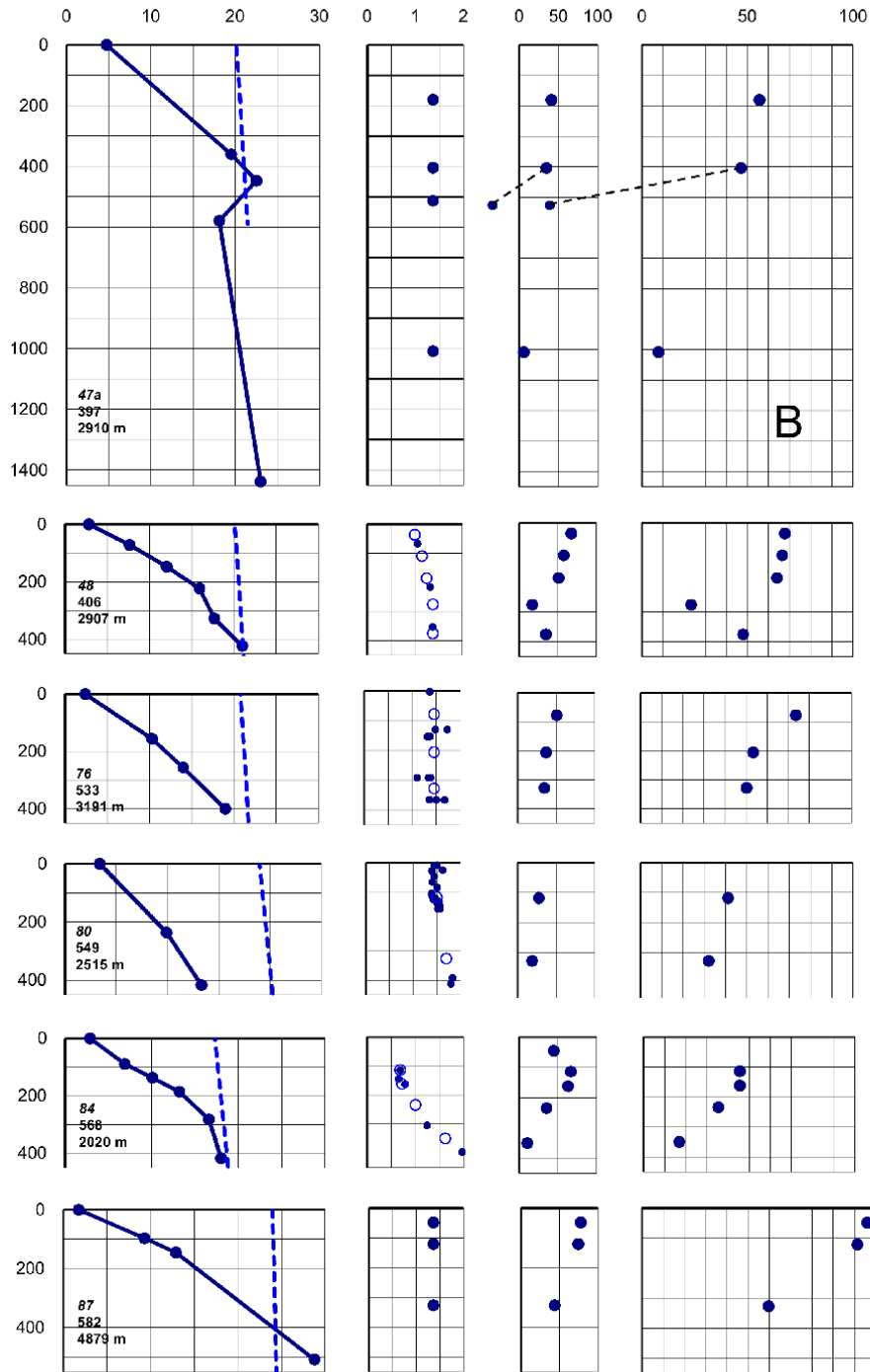
1329

1330

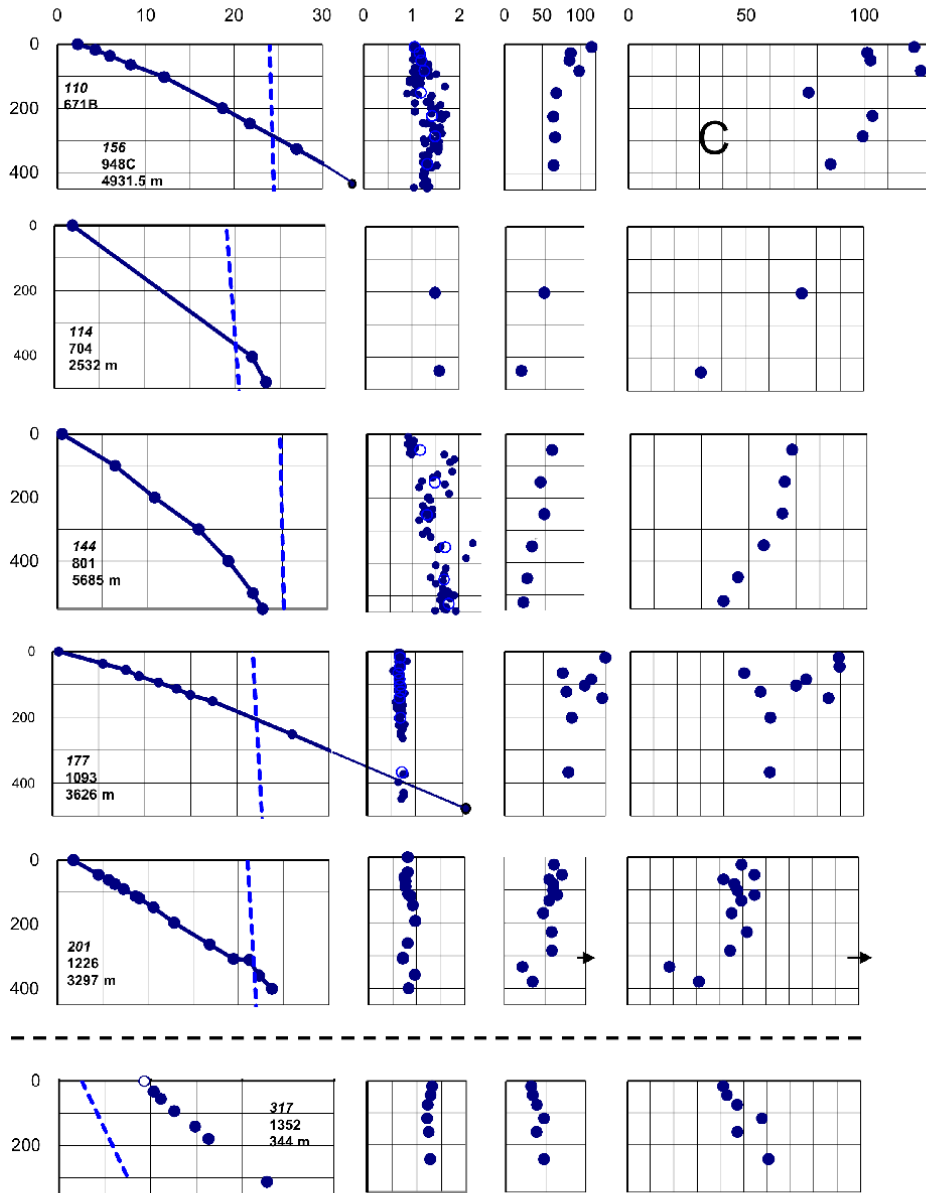
1331 Fig. 2a



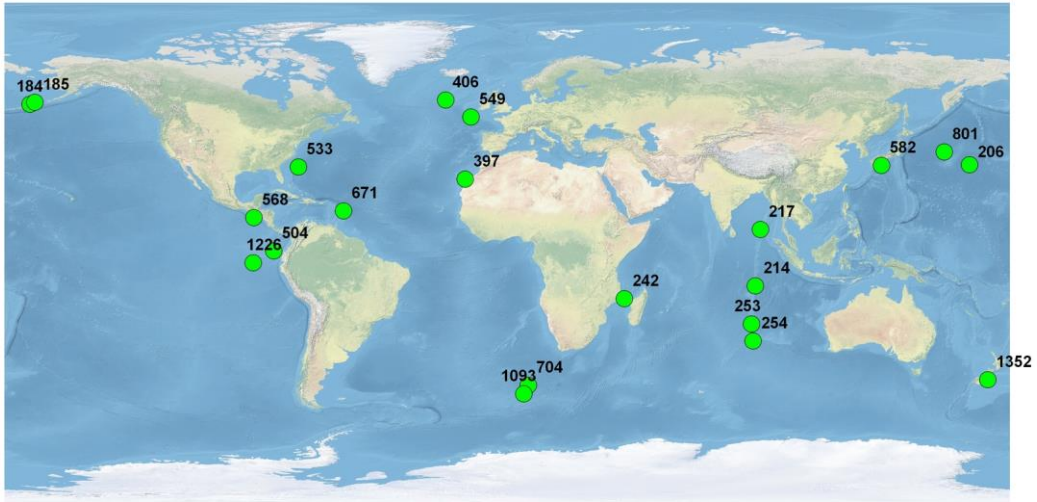
1333 Fig 2b



1335 Fig 2c

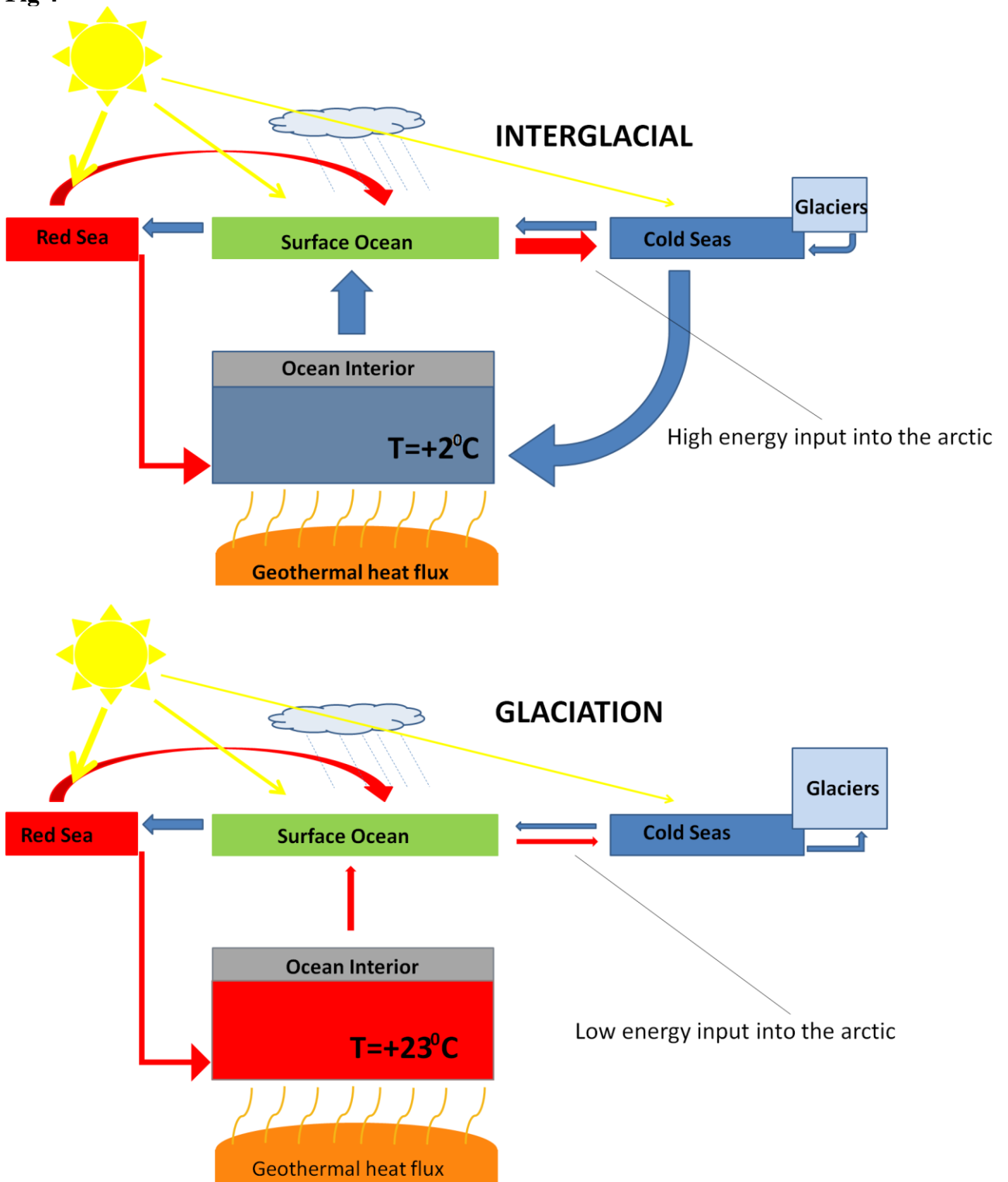


1337 **Fig 3**



- 1338
- 1339
- 1340
- 1341
- 1342
- 1343
- 1344
- 1345
- 1346
- 1347
- 1348
- 1349
- 1350
- 1351
- 1352
- 1353
- 1354
- 1355
- 1356
- 1357
- 1358
- 1359
- 1360
- 1361
- 1362
- 1363
- 1364
- 1365
- 1366
- 1367
- 1368

1369 Fig 4



1370
1371
1372
1373
1374
1375
1376

1377 **Fig 5**

